VOLUME 22 · NUMBER 9 · MAY 1 2004

JOURNAL OF CLINICAL ONCOLOGY

Germ Cell Tumors

CASE 1. Intraocular Metastases From Testicular Cancer

A 23-year-old Japanese man came to the emergency department with headache, vomiting, and visual disturbance in the left eye of 5 days duration. He also had noticed a painless growing right testicular mass 8 months earlier. Physical examination revealed a large mass in the right testis. Neurologic exam was normal except for decreased visual acuity in the left eye. Computed tomography scan of thorax, abdomen, and pelvis showed multiple pulmonary nodules, a large testicular mass, and absence of retroperitoneal lymph node enlargement. Multiple brain lesions as well as a left intraocular mass were seen on magnetic resonance imaging (Fig 1A, 1B). Blood tests showed lactate dehydrogenase 3,094 U/L (normal range, 210 to 410 U/L), human chorionic gonadotropin (HCG) 472,312 U/L and normal alpha-fetoprotein. Inguinal orchiectomy was performed for a testicular tumor measuring 11.0 × 8.5 × 8.0 cm. Pathologic examination revealed mostly seminoma (Fig 2A) with focal choriocarcinoma and embryonal carcinoma components (Fig 2B, anti-HCG antibody). Ophthalmologic examination showed a large mass at the posterior pole in the left eye. Subretinal hemorrhage and serous retinal detachment were also seen (Fig 3). Diagnosis of stage III nonseminomatous germ cell tumor of testis with lung, brain, and intraocular metastases was made. The patient was categorized as having a poor prognosis because of the nonpulmonary visceral metastases and extremely high HCG level. He was treated with bleomycin, etoposide, and cisplatin with concurrent radiotherapy to whole skull and left eye, resulting in complete resolution of cerebral and intraocular lesions, gross residual lung masses, and positive marker. After four courses of bleomycin, etoposide, and cisplatin, he received four courses of salvage chemotherapy with vinblastine, ifosfamide, and cisplatin, resulting in incomplete resolution of bilateral residual lung nodules and negative marker. He subsequently received high-dose chemotherapy consisting of cyclophosphamide, carboplatin, and etoposide followed by autologous peripheral-blood stem-cell rescue.

Testicular germ cell tumor is the most common solid tumor in men between the age of 20 and 35 years. It tends to metastasize to retroperitoneal lymph nodes below renal vessels first, because of the anatomy of lymphatic flow from

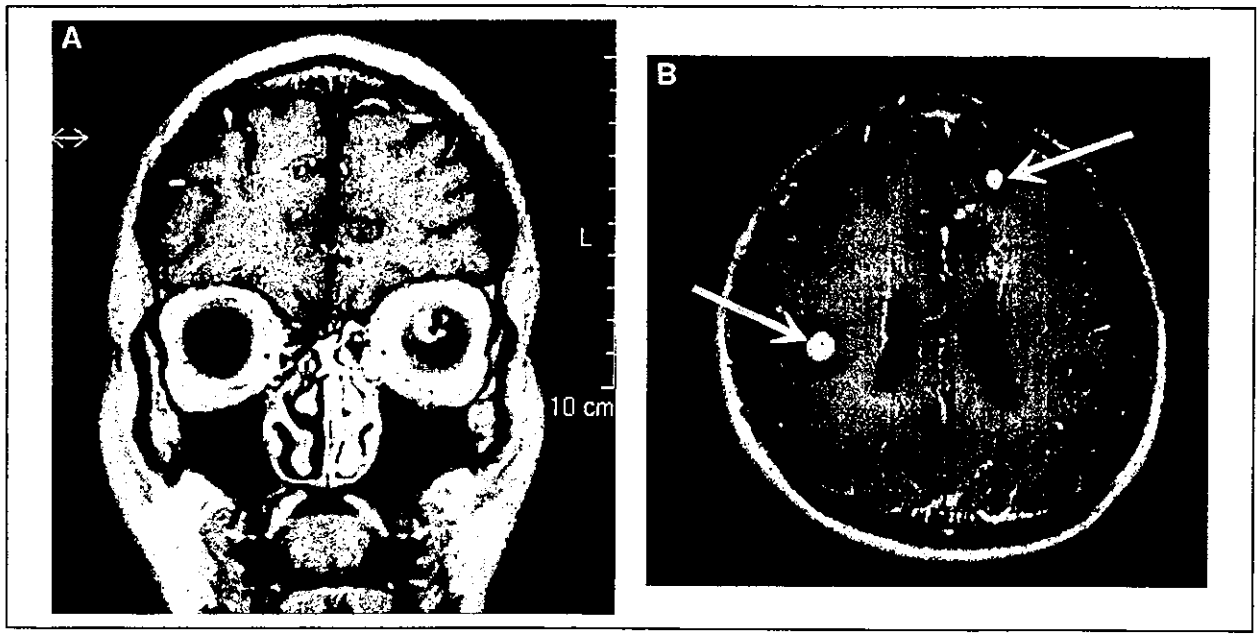

Fig 1.

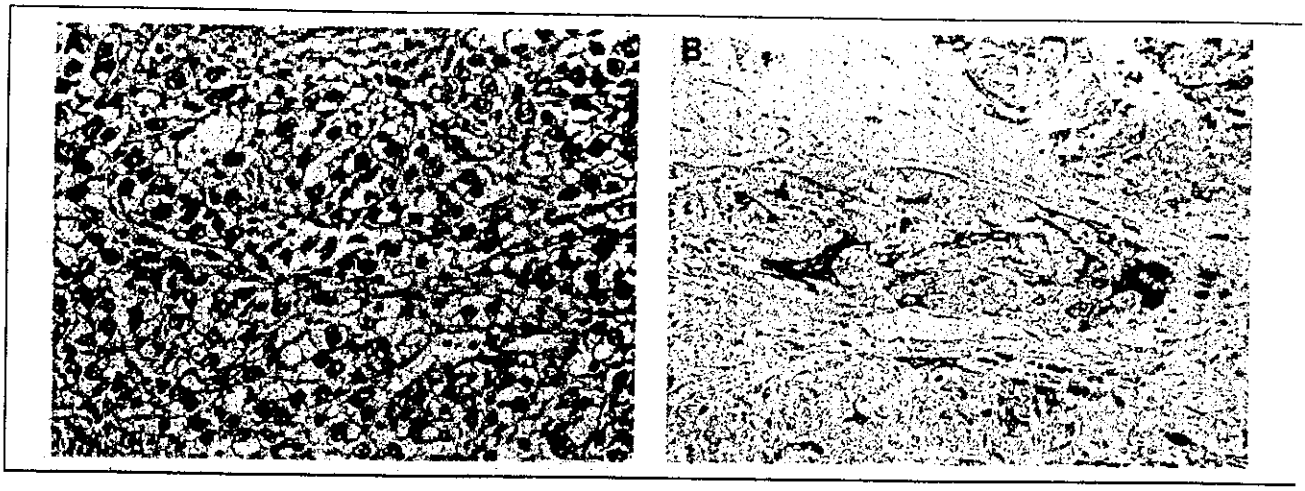

Fig 2.

Fig 3.

testis. It also frequently causes hematogenous spread. Most common visceral site of hematogenous metastasis is lung, followed by liver, brain, and bone. Germ cell tumor is a highly curable disease even with widespread metastases. To standardize the risk stratification of metastatic germ cell tumor, an international germ cell consensus classification was established. High level of tumor marker, mediastinal origin of germ cell tumor, and presence of nonpulmonary visceral metastases are important prognostic factors.[1] Metastatic cancer to the eye was considered to be a rare disease, historically. Approximately 300 patient cases of intraocular metastases from various types of cancer were reported by 1950.[2] Since then, the number of patient cases with intraocular metastases has progressively increased as a result of the improved detection and prolongation of life in patients with widespread metastatic cancer. It is now believed that metastatic cancer to the uvea is the most common form of intraocular malignancy. The proportion of patients with intraocular metastasis among dying patients of all types of cancer was estimated to be 4%.[3] This estimate translates that more than 20,000 patients who would die from cancer would have ocular metastasis annually in the United States. Most intraocular metastases are carcinoma.[4] Breast cancer accounts for the majority, followed by lung cancer[5], and then gastrointestinal cancer.

There have been only a few reports describing intraocular metastases from testicular cancer or germ cell tumor. One is a 4-year-old boy with adenocarcinoma of the testis.[6] Two patient cases of placental and mediastinal choriocarcinoma were reported.[7,8] Recently, a patient with intraocular metastasis from testicular choriocarcinoma was treated successfully with chemotherapy and radiation with cure.[9] Review of the literature suggests that choriocarcinoma accounts for most of intraocular metastases from the germ cell tumor.[7-9] Our patient had a component of choriocarcinoma in the resected specimen. With his high HCG level and propensity of hematogenous spread of choriocarcinoma, his intraocular mass might have shown mostly choriocarcinoma.

Hikaru Nakajima, Masayuki Oki, Shuji Matsukura, Masato Nakamura, Masatoshi Tokunaga, and Kiyoshi Ando

Division of Hematology/Medical Oncology, Departments of Medicine, Ophthalmology, Pathology, and Urology, Tokai University School of Medicine, Isehara, Japan

Authors' Disclosures of Potential Conflicts of Interest

The authors indicated no potential conflicts of interest.

REFERENCES

1. International Germ Cell Consensus Classification: A prognostic factor-based staging system for metastatic germ cell cancers: International Germ Cell Cancer Collaborative Group. J Clin Oncol 15:594-603, 1997

2. Greear JN: Metastatic carcinoma of the eye. Am J Ophthalmol 33:1015-1025, 1950

3. Nelson CC, Hertzberg BS, Klintworth GK: A histopathologic study of 716 unselected eyes in patients with cancer at the time of death. Am J Ophthalmol 95:788-793, 1983

4. Ferry AP, Font RL: Carcinoma metastatic to the eye and orbit: I. A clinicopathologic study of 227 cases. Arch Ophthalmol 92:276-286, 1974

5. Shields CL, Shields JA, Gross NE, et al: Survey of 520 eyes with uveal metastases. Ophthalmology 104:1265-1276, 1997

6. Goldstein I, Wexler D: Metastasis in the choroid from adenocarcinoma of testis. Arch Ophthalmol 13:207-211, 1935

7. Lahav M, Berkowitz S, Albert DM: Primary mediastinal choriocarcinoma in a male metastatic to the choroid. Albrecht Von Graefes Arch Klin Exp Ophthalmol 206:191-197, 1978

8. Barondes MJ, Hamilton AM, Hungerford J, et al: Treatment of choroidal metastasis from choriocarcinoma: Case report. Arch Ophthalmol 107: 796-798, 1989

9. Zech JC, Subiger L, Chiquet C, et al: Testicular choriocarcinoma metastatic to the choroid. Retina 19:164-165, 1999

DOI: 10.1200/JCO.2004.07.187

CASE 2. Unusual Course of Pure Testicular Seminoma

A 33-year-old white man sought medical advice concerning abdominal pain that had lasted a month. He had no significant other medical history. Physical and laboratory evaluation was unremarkable. Ultrasound evaluation showed an enlarged abdominal lymph node. Computed tomography (CT) scan confirmed a 10-mm interaortocaval lymph node without any other abnormal image. Symptoms resolved within hours of treatment with analgesics. The patient was seen 1 month later with recurrent abdominal pain. His new CT scan showed an enlargement of the lymph node to 25 mm. Testicular ultrasound depicted a heterogeneous right testicle, consistent with a testicular tumor. Alpha-fetoprotein, human chorionic gonadotrophin (HCG), free beta-HCG, and lactate dehydrogenase (LDH) levels were normal. A right orchidectomy was performed. The histopathologic diagnosis was a typical pure seminoma. He was then treated with four cycles of chemotherapy with etoposide 100 mg/m^2 and cisplatin 20 mg/m^2, days 1 to 5, because of the unusual growth pattern of the involved lymph node. A partial remission was attained, with shrinkage of the lymph node to 12.5 mm. Close clinical and radiologic follow-up was initiated. Six months later, the lymph node image had enlarged to 30 mm. Excision of the involved retroperitoneal lymph node was performed and pathologic results revealed only necrosis with no viable tumor.

The patient missed follow-up appointments and presented 7 months later with painful abdominal swelling, anorexia, and fatigue. Physical examination revealed massive hepatomegaly. The alkaline phosphatase level was 363 U/L (normal < 135 U/L), gamma-glutamyltransferase level was 361 U/L (normal < 64 U/L), AST level was 223 U/L (normal < 42 U/L), and total bilirubin was 31 μmol/L (normal < 17 μmol/L). The serum LDH level was 10,000 U/L (normal < 600 U/L). Alpha-fetoprotein as well as HCG and free beta-HCG levels were normal. An abdominal CT scan (Fig 1) showed numerous liver metastases as well as portal and celiac lymph node involvement. Thoracic and cerebral CT scans were normal. Ultrasound-guided liver biopsy revealed a typical pure seminoma. Salvage chemotherapy consisting of three cycles of vinblastine, ifosfamide,

Fig 1.

and cisplatin[1] led to the normalization of serum LDH, but only a partial response was obtained on the liver and the lymph node metastases. The patient then was treated with two consecutive cycles of high-dose chemotherapy according to the regimen with ifosfamide 12 g/m^2, carboplatin 1,500 mg/m^2, and etoposide 1,500 mg/m^2,[2] followed by autologous stem-cell transplantation. Consecutive abdominal CT scans showed progressive shrinkage of the liver and lymph node metastases. Additional surgery, including retroperitoneal lymph node dissection and partial hepatectomy, were discussed but not performed because the positron emission tomography scan was normal. At present, the patient is well, with no evidence of disease on CT scan (Fig 2), 24 months after the end of salvage chemotherapy.

Poor-prognosis early-stage seminoma is unusual. Radiotherapy remains the standard treatment for early-stage (stage I and IIA-B, American Joint Committee on Cancer and International Union Against Cancer 1997 classification[3]) pure seminoma. However, this patient's management with chemotherapy according to the advanced seminoma reference protocol[4] was a result of the rapid tumor growth pattern. Retroperitoneal lymph node dissection was not performed after initial chemotherapy in accordance with guidelines regarding the treatment of advanced seminoma.[5] Unlike nonseminomatous germ cell tumors, semi-

ARTICLE

doi:10.1016/j.ymthe.2004.07.029

Competitive Repopulation Assay of Two Gene-Marked Cord Blood Units in NOD/SCID/γc^{null} Mice

Takashi Yahata,[1,2] Kiyoshi Ando,[1,2,*] Hiroko Miyatake,[1] Tomoko Uno,[1] and Tadayuki Sato[1] Mamoru Ito[3] Shunichi Kato[1,4] Tomomitsu Hotta[1,2]

[1]*Division of Hematopoiesis, Research Center for Regenerative Medicine,* [2]*Department of Hematology, and* [4]*Department of Cell Transplantation & Regenerative Medicine, Tokai University School of Medicine, Isehara, Kanagawa 259-1193, Japan*

[3]*Central Institute for Experimental Animals, Kawasaki, Kanagawa 216-0001, Japan*

[*]*To whom correspondence and reprint requests should be addressed at the Department of Hematology, Tokai University School of Medicine Bohseidai, Isehara, Kanagawa 259-1193, Japan. Fax: +81 463 92 4511. E-mail: andok@keyaki.cc.u-tokai.ac.jp.*

Available online 2 September 2004

In multiunit cord blood transplantation, hematopoietic stem cells from each unrelated cord blood (UCB) unit competitively reconstitute the hematopoietic system in a recipient. To evaluate the fate of the progeny of each UCB unit and to determine the effects of graft-versus-graft reaction, we established a novel competitive repopulation assay using NOD/SCID/γc^{null} mice in which human T lymphocytes develop from CD34$^+$ cells. CD34$^+$ cells from each UCB unit were labeled with recombinant lentivirus vectors carrying genes encoding either enhanced green fluorescent protein (EGFP) or enhanced yellow fluorescent protein (EYFP). Hematopoietic chimerism composed of both EGFP$^+$ and EYFP$^+$ cells was stably maintained up to 6 months after transplantation with purified CD34$^+$ cells; the ratio of EGFP$^+$ to EYFP$^+$ cells in peripheral blood and bone marrow posttransplantation was equivalent to the ratio of these cells at transplantation. However, when mononuclear cells from two UCB units were cotransplanted with CD34$^+$ cells, engraftment was highly competitive, with cells from only one or the other of the two UCB units surviving. Further subfractionations of mononuclear cells indicate that the skewed chimerism that is often observed in clinical multiunit cord blood transplantation may be mediated by the cooperation of both CD4$^+$ and CD8$^+$ T cells. The assay established here will be a useful tool for analyzing hematopoietic reconstitution in clinical multiunit cord blood transplantation.

Key Words: gene marking, lentivirus, hematopoietic stem cell, SCID mouse-repopulating cell assay, multiunit cord blood transplantation, NOG mouse, competitive repopulation assay

Introduction

Cord blood (CB) is a potentially rich alternate source of hematopoietic stem cells (HSCs) and progenitors for clinical allogeneic transplantation [1,2]. Despite some promising outcomes with unrelated cord blood transplantation (UCBT) in pediatric recipients, the low cell content of the graft relative to recipient size may adversely affect both the time to hematopoietic recovery and survival [3–6]. Therefore, the major limitation to the widespread use of unrelated CB (UCB) as a source of HSC for transplantation, particularly in adults, is the low yield of stem cells. To overcome this, several centers have initiated multiunit UCBT (m-UCBT) in which two or more units of closely HLA-matched UCB are transplanted [7–9].

In clinical m-UCBT, HSCs from multiple UCB units competitively reconstitute the hematopoietic and immune systems, raising the possibility of a graft-versus-graft reaction or of multiple graft-versus-host reactions. Although an *in vivo* competitive repopulation assay has been widely used in mice [10–12], dogs [13], and nonhuman primates [14,15] to evaluate the potency of HSCs for hematopoietic reconstitution, there is currently no practical assay system for competitive repopulation by human HSCs, which might help to predict the results of graft-versus-graft reactions and immune reconstitution by multiple UCBs.

Xenogeneic transplantation models, in particular the severe combined immunodeficient (SCID) mouse-repopulating cell assay, have been used to evaluate *in vivo* human HSC activity, such as self-renewal and multilineage differentiation [16–19]. The nonobese diabetic (NOD)/SCID mice and related strains have

1525-0016/$30.00

been available for competitive repopulation assay of human HSCs, but a major shortcoming of the NOD/SCID mouse is a lack of reproducible T cell differentiation from $CD34^+$ cells [20–22]. We recently reported that the NOD/SCID/γc^{null} (NOG) mouse, which had been crossed with mice expressing a form of the IL-2Rγ chain lacking the cytoplasmic region, reproducibly develops human T cells, in addition to myeloid, NK, and B-lymphoid cells when transplanted with cord blood $CD34^+$ cells [23–25]. The repopulated T cells bear polyclonal $\alpha\beta$ TCR and respond not only to mitogenic stimuli, such as PHA and IL-2, but also to allogeneic human cells. These results indicate that functional human T lymphocytes can be reconstituted from $CD34^+$ cells in NOG mice. These animals therefore provide a new system in which it is possible to analyze *in vivo* competitive repopulation of the full lymphopoietic system using human HSCs.

Here, we report a novel competitive repopulation system, in which two UCB units were labeled with recombinant lentiviral vectors carrying either an enhanced green fluorescent protein (EGFP)- or an enhanced yellow fluorescent protein (EYFP)-encoding gene to enable easy identification of progeny cells. Using this system, we evaluated competitive repopulation by purified $CD34^+$ cells from two units of UCB with or without cotransplantation of mononuclear cells (MNC) and their purified populations.

Results

Competitive Repopulation of Combined UCB $CD34^+$ Cells Transplanted into the NOG Mouse

We transplanted 11 pairs of UCB $CD34^+$ cells bearing distinct HLA alleles simultaneously into sublethally irradiated NOG mice (Table 1). To distinguish progeny derived from each UCB unit of $CD34^+$ cells, we labeled one unit by transfection with a lentivirus vector containing the EGFP gene and the other unit with a lentivirus vector containing the EYFP gene. After transplantation, we collected peripheral blood (PB) cells retro-orbitally at various intervals and analyzed them by flow cytometry for the presence of human hematopoietic cells expressing the leukocyte common antigen CD45 (Figs. 1A and 1B). Individual progeny from each unit of UCB $CD34^+$ cells were easily identified by the expression of these marker genes.

To evaluate the stability of any chimerism from two UCB donors in mice, we plotted the ratio of $EGFP^+$ to $EYFP^+$ cell number in PB over time after transplantation. Although the transduction efficiencies and numbers of $CD34^+$ cells varied between each experiment, the chimeric ratio of $EGFP^+$ to $EYFP^+$ cells observed at 3 weeks after transplantation was fairly stable up to at least 18 weeks (Fig. 1C). In some experiments, the ratio was stable up to 6 months after transplantation ($n = 3$ analyzed, data not shown).

To evaluate the relative viability of the two UCB donors in mice, we plotted the ratio of $EGFP^+$ to $EYFP^+$

TABLE 1: Characteristics of the CB units

Expt	No. cells ($\times 10^4$)	$CD34^+CD38^-$ (%)	Infection	Transduction efficiency (%)	HLA A	HLA B	HLA DR
1	5.5	10.99	GFP	12.72	2/26	46/60	8/–
	11.4	8.7	YFP	12.11	2/–	51/75	15/–
2	11	5.86	GFP	17.04	1/24	37/52	14/15
	8	4.56	YFP	16.72	2/24	7/35	1/4
3	13.8	10.21	GFP	14.84	24/–	7/61	1/9
	16	4.8	YFP	15.13	2/24	46/–	8/–
4	15.8	4.35	GFP	7.56	24/33	44/52	9/13
	10.5	5.67	YFP	8.13	1/24	37/52	10/15
5	19	6.37	GFP	18.64	2/24	46/62	4/8
	13.9	4.1	YFP	17.87	24/26	7/61	9/13
6	17.5	8.39	GFP	18.76	N.D.	N.D.	N.D.
	24	6.22	YFP	17.81	2/–	59/61	4/–
7	8.75	13.14	GFP	10.35	2/24	35/62	4/11
	4	5.24	YFP	15.84	2/33	51/–	8/9
8	9	14.58	GFP	28.16	24/26	52/62	4/15
	35	5.4	YFP	25.58	2/24	46/61	8/9
9	98	7.57	GFP	25.28	24/33	7/44	1/13
	47	6.84	YFP	26.63	24/–	52/61	9/15
10	18.75	9.24	GFP	25.20	24/26	54/61	4/9
	15.75	4.55	YFP	12.55	11/24	51/62	11/15
11	10.5	17.6	GFP	27.01	24/33	44/52	9/13
	9.5	12.53	YFP	23.84	1/24	37/52	10/15

N.D., not determined. –, blank allele.

doi:10.1016/j.ymthe.2004.07.029

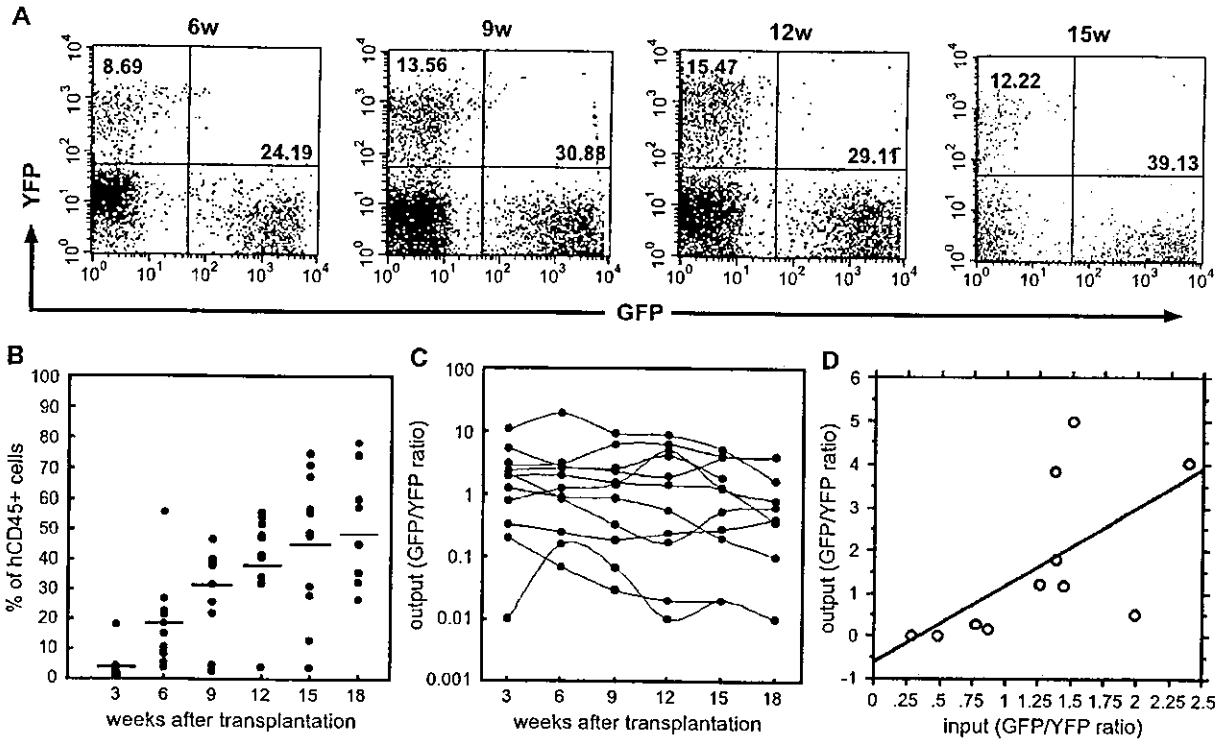

FIG. 1. (A) Representative FACS profiles of competitive repopulation of EGFP- or EYFP-transduced CB CD34$^+$ cells in an individual NOG mouse recipient. PB cells were collected at specific intervals and stained with anti-human CD45 mAb. The stained cells were then analyzed by flow cytometry gated for the expression of CD45. Each donor-derived human hematopoietic cell was distinguished by the expression of the marker EGFP or EYFP. (B) Kinetics of human hematopoietic cells in NOG mice transplanted with two units of CB CD34$^+$ cells. PB cells were collected at various intervals from transplanted NOG mice (n = 11) and stained with anti-human CD45 mAb. Each dot represents one mouse recipient, and bars indicate the average of engraftment. (C) The ratio of each donor's derived CD45$^+$ hematopoietic cells detected in the NOG mouse PB was calculated. (D) A weak linear relationship between the ratio of injected CD34$^+$ cell number (horizontal axis) and the ratio of human hematopoietic cells engrafted in the PB at 15 weeks after transplantation (vertical axis) (r = 0.623, n = 11, P = 0.039).

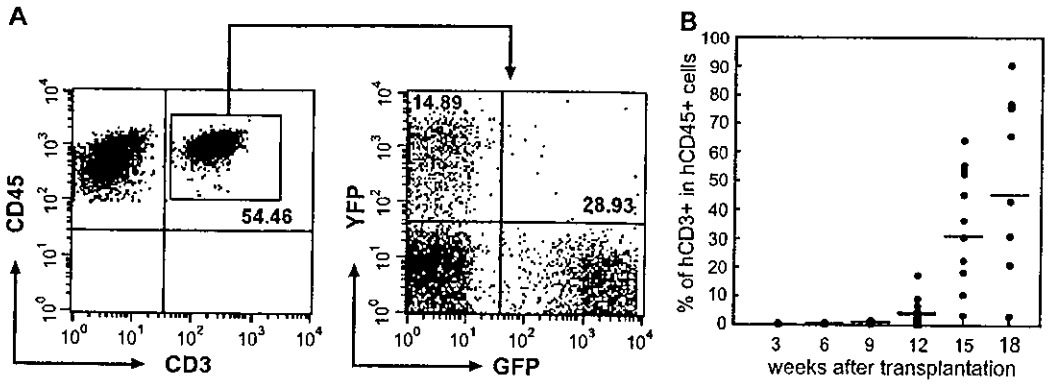

FIG. 2. (A) Representative FACS profiles of CD3$^+$ T lymphocytes in competitive repopulation of EGFP- or EYFP-transduced CB CD34$^+$ cells in an individual NOG mouse recipient. PB cells were collected at 15 weeks after transplantation. Anti-human CD3 mAb and anti-human CD45 mAb were used to detect human T lymphocytes in the PB of engrafted NOG mice. The CD3$^+$CD45$^+$ region was gated and marker gene expression was analyzed. (B) Kinetics of human CD3$^+$ T lymphocytes in NOG mice transplanted with two units of CB CD34$^+$ cells. PB cells were collected at various intervals from transplanted NOG mice (n = 11) and stained with anti-human CD3 mAb and anti-human CD45 mAb. The stained cells were then analyzed by flow cytometry gated for the expression of CD45. Each dot represents one mouse recipient, and bars indicate the average engraftment.

TABLE 2: Lineage analysis of T lymphocytes derived from two UCB units in the thymus of NOG mice

Expt	Phenotype	Lineages (%) DN	DP	$CD4^+$ SP	$CD8^+$ SP
1	$GFP^+/CD45^+$	N.D.	N.D.	N.D.	N.D.
	$YFP^+/CD45^+$	N.D.	N.D.	N.D.	N.D.
3	$GFP^+/CD45^+$	4.11	69.08	14.09	12.72
	$YFP^+/CD45^+$	3.86	66.80	16.22	13.13
4	$GFP^+/CD45^+$	8.00	50.50	26.00	15.50
	$YFP^+/CD45^+$	1.60	65.07	21.60	18.16
6	$GFP^+/CD45^+$	8.90	44.70	27.35	22.72
	$YFP^+/CD45^+$	1.96	67.99	18.22	11.83
7	$GFP^+/CD45^+$	15.17	45.07	18.16	21.6
	$YFP^+/CD45^+$	18.20	43.80	17.22	20.78
9	$GFP^+/CD45^+$	32.64	34.55	12.81	19.99
	$YFP^+/CD45^+$	22.32	20.06	16.47	41.15
10	$GFP^+/CD45^+$	2.03	35.29	28.26	34.42
	$YFP^+/CD45^+$	0.24	44.01	20.45	35.30
11	$GFP^+/CD45^+$	16.55	51.39	18.39	16.55
	$YFP^+/CD45^+$	0.29	38.07	24.08	37.56

N.D., not determined.

cell number in PB against the ratio of engrafted $CD34^+$ cells. There was a linear relationship between the $EGFP^+$ to $EYFP^+$ cell ratio observed at 15 weeks after transplantation and the $EGFP^+$ to $EYFP^+$ $CD34^+$ cell ratio at the time of transplantation ($r = 0.623$, $P = 0.039$, $n = 11$; Fig. 1D). Similarly, the $EGFP^+$ to $EYFP^+$ ratio in engrafted cells in bone marrow (BM) correlated with the $EGFP^+$ to $EYFP^+$ ratio at transplantation ($r = 0.713$, $P = 0.0458$, $n = 8$), although three mice died before the analysis.

These data demonstrate that one unit of UCB $CD34^+$ cells will engraft with the same efficiency in NOG mice regardless of whether a second, different, unit of UCB $CD34^+$ cells is simultaneously transplanted.

Multilineage Differentiation of Two Units of Cord Blood $CD34^+$ cells

Consistent with our previous results [23], we began to detect human $CD3^+$ T lymphocytes at 9 weeks posttransplantation of UCB $CD34^+$ cells and their numbers steadily increased up to 18 weeks (Fig. 2B). Both $EGFP^+$ and $EYFP^+$ $CD3^+$ T lymphocytes were detected in PB of NOG mice between 9 and 18 weeks posttransplantation (Fig. 2A).

Fifteen to 24 weeks after transplantation, we killed the mice and collected the thymus, BM, and spleen to analyze the progeny of the two units of UCB $CD34^+$ cells. In the thymus, most thymocytes in the NOG mice were human $CD3^+$ cells, which had differentiated from both $EGFP^+CD34^+$ cells and $EYFP^+CD34^+$ cells (Table 2 and Fig. 3). Thymocytes from both donors showed normal differentiation patterns, which comprised both double-positive and single-positive subsets of CD4/CD8.

In BM and spleen, we analyzed multilineage differentiation of $EGFP^+CD34^+$ cells and $EYFP^+CD34^+$ cells by gating $EGFP^+CD45^+$ and $EYFP^+CD45^+$ cells. In addition to $CD3^+$ T cells, $CD19^+$ B cells, $CD56^+$ NK cells, $CD14^+$ monocytes, $CD33^+$ myeloid cells, and primitive $CD34^+$ cells arose from both the $EGFP^+CD45^+$ and the $EYFP^+CD45^+$ units (Table 3, Fig. 4, and spleen data not shown).

These data demonstrate that the multilineage engraftment of one unit of UCB $CD34^+$ cells in NOG mice is

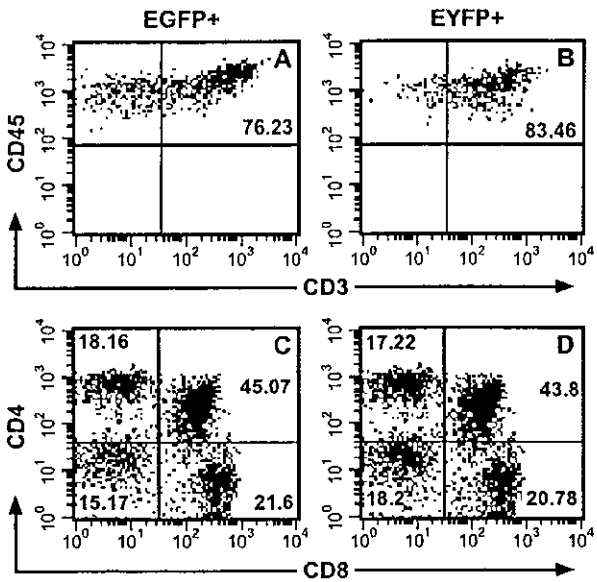

FIG. 3. Representative FACS analysis of human T cell engraftment in the thymus of a NOG mouse recipient transplanted with two combined units of CB $CD34^+$ cells. At 18 weeks after transplantation, thymocytes were collected and stained with anti-human CD45 mAb. Each (A, C) $CD45^+EGFP^+$ and (B, D) $CD45^+EYFP^+$ region was gated, and the expression of (A, B) CD3 and (C, D) CD4/CD8 was analyzed. The relative frequencies of each population are indicated.

doi:10.1016/j.ymthe.2004.07.029

TABLE 3: Lineage analysis of two UCB units of CD34⁺-derived hematopoietic cells that had differentiated in BM of NOG mice

Expt	Phenotype	Lineages (%) CD14⁺	CD19⁺	CD33⁺	CD34⁺	CD56⁺
1	GFP⁺/CD45⁺	11.76	38.46	37.27	15.91	4.00
	YFP⁺/CD45⁺	12.22	57.47	19.54	12.05	2.33
3	GFP⁺/CD45⁺	16.28	34.34	38.26	14.01	4.35
	YFP⁺/CD45⁺	18.24	25.07	49.22	16.47	8.13
4	GFP⁺/CD45⁺	9.21	21.37	10.16	10.29	0.88
	YFP⁺/CD45⁺	10.76	29.86	12.63	10.72	1.61
6	GFP⁺/CD45⁺	24.44	11.18	37.77	3.36	4.75
	YFP⁺/CD45⁺	10.97	46.70	13.52	5.86	8.04
7	GFP⁺/CD45⁺	17.17	62.97	28.72	18.91	1.32
	YFP⁺/CD45⁺	12.85	48.52	20.42	9.49	2.55
9	GFP⁺/CD45⁺	5.25	18.37	11.13	6.44	6.17
	YFP⁺/CD45⁺	17.19	37.23	31.25	6.60	7.23
10	GFP⁺/CD45⁺	5.33	24.63	10.65	3.22	2.98
	YFP⁺/CD45⁺	3.06	18.24	3.70	3.93	2.67
11	GFP⁺/CD45⁺	10.78	52.72	13.51	3.90	2.25
	YFP⁺/CD45⁺	26.24	29.46	7.44	9.76	1.06

stable and unaffected by lymphopoietic repopulation by another UCB unit.

Effects of Cotransplantation of CD34⁻ Mononuclear Cells on Competitive Repopulation in The NOG Mouse

Unfractionated UCB cells containing mature immune-competent cells are commonly used in clinical UCBT. These cells can induce graft-versus-host, graft-versus-tumor, and graft-versus-graft reactions. The effects of the latter reaction on engraftment in particular are poorly understood in m-UCBT. To assess these effects, we performed three sets of competitive repopulation assay by cotransplantation of pairs of CD34⁻ MNC with EGFP⁺CD34⁺ cells and EYFP⁺CD34⁺ cells (Table 4).

Four to 6 weeks posttransplantation, we sacrificed the mice and analyzed the ratio of engrafted EGFP⁺CD45⁺ and EYFP⁺CD45⁺ cells in BM MNC by flow cytometry. When only purified CD34⁺ cells were transplanted, both UCB units engrafted as expected. However, when CD34⁻ MNCs were cotransplanted with CD34⁺ cells, only CD45⁺ cells from one or the other UCB engrafted in all mice analyzed (Fig. 5). These results indicate that CD34⁻ MNC from one UCB somehow inhibited engraftment of cells from the other UCB.

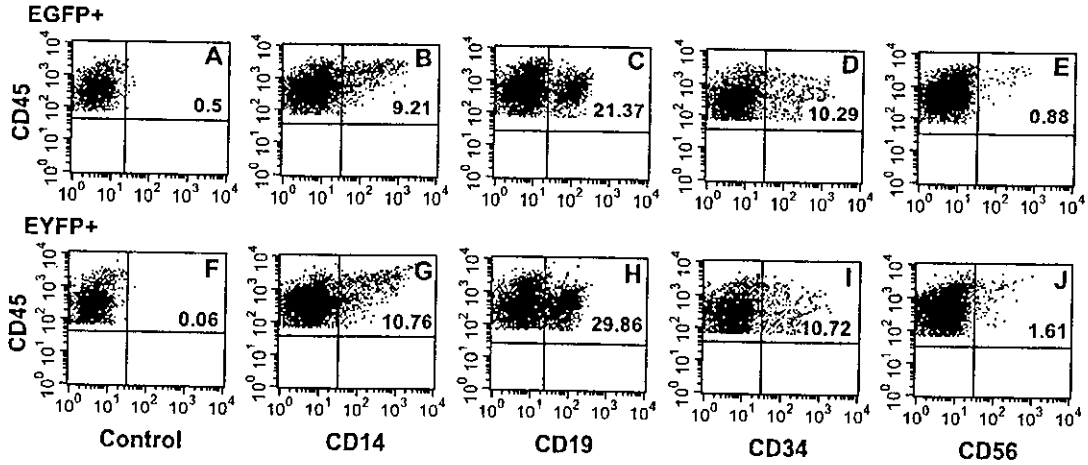

FIG. 4. Representative FACS profile of human multilineage engraftment in a NOG mouse recipient transplanted with two combined units of CB CD34⁺ cells. At 18 weeks after transplantation, BM cells were collected and analyzed for multilineage differentiation of engrafted human hematopoietic cells. To distinguish hematopoietic cells derived from each donor, each (A–E) CD45⁺EGFP⁺ and (F–J) CD45⁺EYFP⁺ region was gated, and the percentage of human CD45⁺ cells expressing the respective surface markers was measured. Human lineage-specific mAbs were used to detect (B, G) myeloid CD45⁺CD14⁺, (C, H) lymphoid CD45⁺CD19⁺, (E, J) CD45⁺CD56⁺, and (D, I) immature CD34⁺ progenitor cells in the marrow of engrafted NOG mice. The relative frequencies of each population are indicated.

TABLE 4: Characteristics of purified CD34⁺ cells and MNCs in each CB unit

Expt	Infection	CD34⁺/mouse (×10⁴)	MNC/mouse (×10⁶)	HLA A	HLA B	HLA DR	HLA DRw
1	GFP	6.0	7.4	2/–	59/61	4/–	53/–
	YFP	6.0	8.8	2/24	51/67	9/12	52/53
2	GFP	12	1.0	2/24	7/51	1/9	53/–
	YFP	7.3	1.0	24/33	44/75	4/13	52/53
3	GFP	16	1.0	24/–	60/–	11/13	52/–
	YFP	11	1.0	2/24	7/61	1/9	53/–

–, blank allele.

To clarify the cell population responsible for this inhibitory effect, we cotransplanted purified CD4⁺ or CD8⁺ T lymphocytes or CD4/CD8 double-negative (DN) cells with EGFP⁺CD34⁺ cells and EYFP⁺CD34⁺ cells into NOG mice (Table 5). Although CD34⁻ MNCs eliminated either EGFP⁺CD45⁺ or EYFP⁺CD45⁺ cells as expected, there was no inhibition of engraftment of EGFP⁺CD45⁺ or EYFP⁺CD45⁺ cells by purified CD4⁺ or CD8⁺ T lymphocytes or CD4/CD8 double-negative cells in any mice (Fig. 6). These results indicate that a combination of two or more populations of CD4⁺, CD8⁺, and/or DN cells is required for this inhibitory effect.

To determine the effects of a combination of two populations on engraftment, we cotransplanted EGFP⁺CD34⁺ cells and EYFP⁺CD34⁺ cells with combined populations of CD4⁺ and CD8⁺ cells, CD4⁺ and DN cells, and CD8⁺ and DN cells into NOG mice (Table 6). Both CD4⁺ and CD8⁺ cells from one donor cooperated to inhibit engraftment of cells from the other donor, as we observed with whole CD34⁻ MNC cotransplantation (Fig. 7A). There was no inhibition of engraftment of EGFP⁺CD45⁺ or EYFP⁺CD45⁺ cells by the combination of CD4⁺ and DN cells or CD8⁺ and DN cells (Fig. 7B).

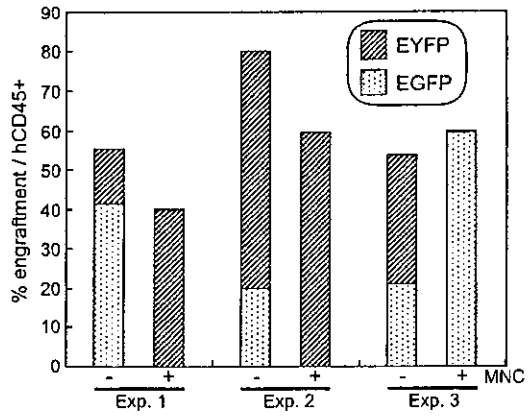

FIG. 5. The effects of CD34⁻ MNCs on competitive repopulation by CD34⁺ cells in the NOG mouse. EGFP- or EYFP-transduced CD34⁺ cells with or without a respective fraction of CD34⁻ MNCs were injected into the same NOG mouse (Table 4). At 4 to 6 weeks after transplantation, the ratio of engrafted donor-derived hematopoietic cells from each unit was measured using the expression of CD45 and the marker genes in flow cytometry. To exclude residual human T cells derived from CD34⁻ MNCs, CD3⁺ cells were gated out at FACS analysis. Data shown are the ratios of CD45⁺EGFP⁺ and CD45⁺EYFP⁺ cells in the BM MNCs of the same NOG recipient (three independent experiments).

Discussion

The possibility of competitive reconstitution of the hematopoietic system by HSCs from multiple UCB units in clinical m-UCBT raises several important questions. Do immune-competent cells developed from two unrelated HSCs affect hematopoietic engraftment or reconstitution in a host? Do mature immune-competent cells derived from two UCB units affect hematopoietic engraftment or reconstitution in a host? To address these questions, we used a novel *in vivo* competitive repopulation system using NOG mice that allows complete reconstitution of human lymphocytes, including T cells, from CD34⁺ UCB that respond to both mitogenic stimuli, such as PHA and IL-2, and allogeneic human cells [23,25].

We demonstrated here that hematopoietic cells derived from two UCB units engrafted stably, even after CD3⁺ T cells were detected in recipient PB at 12 weeks after transplantation, and that the ratio of chimerism between cells derived from the two UCB units was correlated with the ratio of cells at transplantation (Fig. 1). Recently, Kim *et al.* [26] demonstrated that two lineage-depleted UCB units could coengraft in NOD/SCID mice. However, this assay could not assess the effects of an immune system derived from HSCs on engraftment by the other, since T cells did not differentiate from CD34⁺ cells in NOD/SCID mice. Therefore, this is the first demonstration that human immune-competent cells from two immunologically distinct CD34⁺ donor stem cells can develop normally in the same host environment without inhibiting each other. In recipient NOG mouse thymus, both EGFP⁺CD3⁺ and EYFP⁺CD3⁺ cells showed a normal pattern of T cell differentiation, which comprised both double-positive and single-positive CD4/CD8 subsets (Fig. 4 and Table 2). This suggests that there may have been negative selection in the clonal deletion of cells reactive to each other. Therefore, the content of HSCs may be a good predictor of the resultant chimerism in a mouse, as shown in Fig. 1D.

doi:10.1016/j.ymthe.2004.07.029

TABLE 5: Characteristics of purified CD34⁺ cells and effector cells in each CB unit

Expt	Infection	CD34⁺ cells[a]	MNC fraction[b]	HLA A	HLA B	HLA DR	HLA DRw
1	GFP	+	+	2/31	51/54	4/15	51/53
	YFP	+	–	2/33	39/44	9/13	52/53
2	GFP	+	–	11/24	54/67	4/8	53/–[c]
	YFP	+	+	2/24	35/62	9/12	52/53
3	GFP	+	+	2/24	35/61	4/8	53/–
	YFP	+	–	2/26	35/61	9/15	51/53

[a] EGFP- or EYFP-transduced CD34⁺ cells were transplanted into the same NOG mouse (range of transplanted cell dose $6.8–9 \times 10^4$ cells).
[b] Unfractionated MNCs (range $7–10 \times 10^5$ cells), CD4⁺ cells (range $3.3–5 \times 10^5$ cells), CD8⁺ cells (range $1.4–2 \times 10^5$ cells), and CD4/CD8 double-negative fraction (range $2–3 \times 10^5$ cells) were prepared from one CB CD34⁻ fraction (+) and injected into NOG mice together with CD34⁺ cells derived from the same donor and CD34⁺ cells derived from the second unit of CB (–).
[c] –, blank allele.

In clinical m-UCBT, the transplanted whole MNC can induce a rapid graft-versus-graft reaction. One study reported successful engraftment of only 1 of 12 randomly selected units of UCB [7]. Another study demonstrated that only one of the two UCB donors was responsible for hematopoiesis in 16 of 18 patients with sustained engraftment [27]. However, another study found that both of the transplanted UCBs contributed to stable hematopoiesis, and this success was attributed to the grafts being closely matched, with only a single mismatch between them at one HLA-DRB1 allele [8]. In the present study, we observed engraftment of either of mismatched pairs of UCB units (Tables 4 and 5), confirming the utility of this animal model to analyze engraftment and hematopoiesis in m-UCBT. We also observed that graft-versus-graft reaction was associated with the CD34⁻ mononuclear cells in a cord blood unit. In future experiments it would be of interest to analyze the chimerism when an HLA-matched UCB pair is cotransplanted.

One possible drawback to our model is the potential antigenicity of the marker genes EGFP and EYFP used to identify the transplanted cell populations. These two proteins have very similar antigenic properties, since EYFP is simply a mutant form of EGFP [28]; therefore any specific immune reaction would be expected to have an equivalent effect on both cell populations. However, in every case shown in Figs. 5, 6, and 7 either EGFP⁺ or EYFP⁺ cells were eliminated, suggesting that this was due to an allospecific reaction.

To identify further the cell population responsible for graft-versus-graft reaction, we cotransplanted purified populations of CD4⁺, CD8⁺, or DN cells from two UCBs together with CD34⁺ cells, but none of these cell populations alone was sufficient to generate a reaction against the other UCB unit (Fig. 6). This suggests that perhaps two populations of effector cells are needed to induce a graft-versus-graft reaction. Consistent with this, we could reproduce this inhibitory effect on engraftment by CD34⁻ mononuclear cells only when both CD4⁺ and CD8⁺ cells were transplanted simultaneously (Fig. 7). These results support the hypothesis that graft-reactive CD8⁺ CTL served as the terminal effector cell in the rejection, while CD4⁺ cells provided the signals required for CTL development and expansion [29]. As the strongest alloreaction is provoked by major histocompatibility complex (MHC) antigens, T cells recognize the alloantigens either "directly" as foreign antigens or "indirectly" as presented by self-MHC molecules [30,31]. Our results may suggest that CD4⁺ and CD8⁺ T cells from one graft recognized the MHC antigens from the other directly as nonself and then eliminated hematopoietic cells of the other graft, since DN cells were not required as antigen-presenting cells to elicit the reaction. However, Kim and colleagues demonstrated that the mixed transplantation

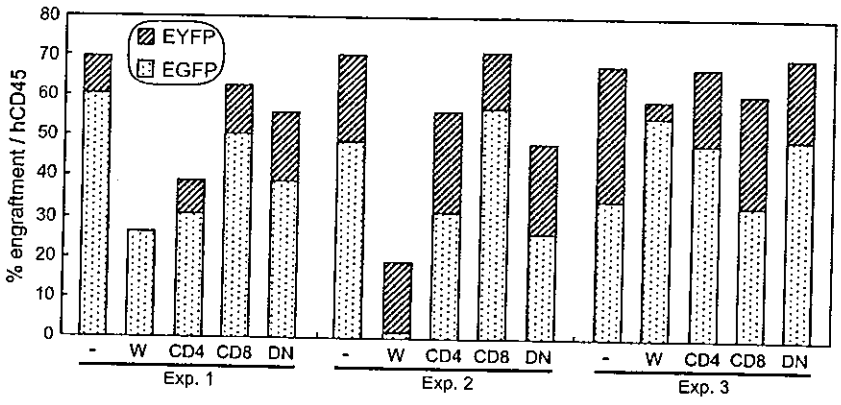

FIG. 6. The effects of fractionated effector cells contained in CD34⁻ MNCs on competitive repopulation by CD34⁺ cells in the NOG mouse. CD4⁺ or CD8⁺ T lymphocytes and the CD4/CD8 double-negative fraction were sorted from one CB CD34 fraction and injected into NOG mice together with CD34⁺ cells derived from the same CB and CD34⁺ cells derived from the second unit of CB (Table 5). At 3 weeks after transplantation, the ratio of engraftment was analyzed by the same method as for Fig. 5. Data shown are the ratios of CD45⁺EGFP⁺ and CD45⁺EYFP⁺ cells in the BM MNCs of the same NOG recipient (three independent experiments). (–) Transplants without CD34⁻ MNCs; (W) transplants with whole CD34⁻ MNC.

TABLE 6: Characteristics of purified CD34$^+$ cells and effector cells in each CB unit

Expt	Infection	CD34$^+$ cells[a]	MNC fraction[b]	HLA A	HLA B	HLA DR	HLA DRw
1	GFP	+	−	2/31	35/−[c]	12/15	51/52
	YFP	+	+	24/26	51/62	4/15	51/53
2	GFP	+	+	2/31	46/61	8/15	51/−
	YFP	+	−	2/24	35/55	4/9	53/−
3	GFP	+	+	24/33	44/75	8/9	53/−
	YFP	+	−	11/−	44/59	4/13	52/53

[a] EGFP- or EYFP-transduced CD34$^+$ cells (5×10^4 cells) were transplanted into the same NOG mouse.
[b] Unfractionated MNCs (10×10^5 cells), CD4$^+$ cells (5×10^5 cells), CD8$^+$ cells (2×10^5 cells), and CD4/CD8 double-negative fraction (range 2–3 $\times 10^5$ cells) were prepared from one CB CD34$^-$ fraction (+). Each fraction were combined as CD4$^+$ and CD8$^+$ cells, CD4$^+$ and DN cells, and CD8$^+$ and DN cells and transplanted into NOG mice together with CD34$^+$ cells derived from the same donor and CD34$^+$ cells derived from the second unit of CB (−).
[c] −, blank allele.

of two allogeneic UCB grafts led to single-donor predominance independent of the degree of HLA compatibility between the two grafts [26]. Further investigation is necessary to determine how CD4$^+$ and CD8$^+$ cells contribute to predominant engraftment of HSCs, through either direct recognition of the MHC antigens or other nonspecific effects.

We have established a novel *in vivo* competitive repopulation assay using a new NOG mouse system that may facilitate study of the behavior of different units of stem cells after transplantation. Furthermore, we clearly demonstrated that the lentiviral gene marking strategy can easily distinguish the two distinct donor cells by flow cytometric analysis, independent of

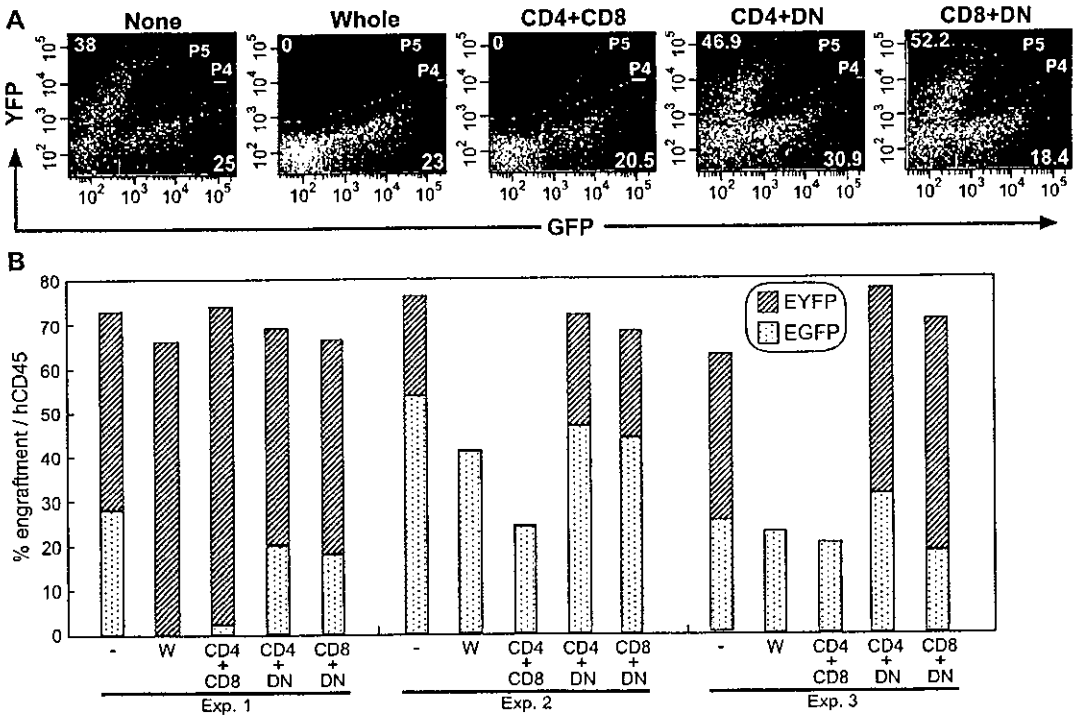

FIG. 7. The effects of combined cell populations contained in CD34$^-$ MNCs on competitive repopulation by CD34$^+$ cells in the NOG mouse. CD4$^+$ and CD8$^+$ T lymphocytes and the CD4/CD8 double-negative fraction were sorted from one CB CD34$^-$ fraction. Each sorted fraction was combined to give CD4$^+$ and CD8$^+$ cells, CD4$^+$ and DN cells, or CD8$^+$ and DN cells and injected into NOG mice together with CD34$^+$ cells derived from the same CB and CD34$^+$ cells derived from the second unit of CB (Table 6). At 3 weeks after transplantation, the ratio of engraftment was analyzed by the same method as for Fig. 5. (A) Representative FACS profiles of competitive repopulation of EGFP- or EYFP-transduced CB CD34$^+$ cells in an individual NOG mouse recipient. (B) Summary of three independent experiments. Data shown are the ratios of CD45$^+$EGFP$^+$ and CD45$^+$EYFP$^+$ cells in the BM MNCs of the same NOG recipient. (−) Transplants without CD34$^-$ MNCs; (W) transplants with whole CD34$^-$ MNC.

doi:10.1016/j.ymthe.2004.07.029

cell surface antigens, expression of intracellular isoenzymes, or hemoglobin subtypes. This strategy is also useful for the examination of the stem cell competitive repopulation activity of variety cell sources such as BM cells and cord blood cells, *ex vivo* expanded cells, and nonexpanded cells. Gene transduction by lentiviral infection did not have any apparent untoward effects on the behavior of HSCs, such as multilineage differentiation and long-term repopulation.

We hope that the *in vivo* assay system described here will be useful, not only for examining the competitive hematopoietic repopulation from multiple UCB units, but also for predicting the effects of MNCs cotransplanted in clinical m-UCBT. To evaluate the relevance of this system as a surrogate human HSC assay, it will be important to correlate the results of engraftment in this model with engraftment in clinical m-UCBT.

Materials and Methods

Cells. CB samples were obtained from full-term deliveries following institutional guidelines approved by the Tokai University Committee on Clinical Investigation. MNCs were isolated by Ficoll–Hypaque (Lymphoprep, 1.077 ± 0.001 g/ml; Nycomed, Oslo, Norway) density gradient centrifugation. Cells were washed and suspended in phosphate-buffered saline (PBS) containing 0.1% of human serum globulin (Sigma, St. Louis, MO, USA). $CD34^+$ cell fractions were prepared from Ficoll-separated MNCs using the CD34 Progenitor Cell Isolation Kit (Miltenyi Biotec, Sunnyvale, CA, USA) according to the manufacturer's directions. The enriched $CD34^+$ cell fraction was stained either with fluorescein isothiocyanate (FITC)-conjugated anti-CD34 mAb (581; Coulter/Immunotech, Marseille, France) or with allophycocyanin (APC)-conjugated anti-CD3 mAb (UCHT1; Coulter/Immunotech). $CD34^+CD3^-$ cells were sorted using a FACSVantage flow cytometer (BD Biosciences, San Jose, CA, USA) equipped with HeNe and argon lasers. This resulted in a highly purified $CD34^+$ cell fraction (more than 99%) in which no $CD3^+$ cells were detected on FACS analysis. Sorted $CD34^+CD3^-$ cells were cryopreserved in liquid nitrogen until use. Column passthrough $CD34^-$ MNC fractions were also cryopreserved. On the day of transplantation, cryopreserved $CD34^-$ MNC fractions were thawed and stained with PE-conjugated anti-CD4 (SK3) and FITC-conjugated anti-CD8 (SK1) mAbs (all BD Biosciences). Stained cells were sorted using the FACSVantageSE Diva option (BD Biosciences) gated on each $CD4^+CD8^-$, $CD4^-CD8^+$, and $CD4^-CD8^-$ region. Purified populations were >98% pure. Dead cells stained with PI were excluded from the analysis. The HLA of each CB unit was determined by molecular typing using a Micro SSP HLA Classes I and II ABDR DNA Typing Tray (One Lambda, Canoga Park, CA, USA).

Lentivirus infection. Transduction of the EGFP or its yellow variant EYFP gene into $CD34^+$ cells by recombinant lentivirus infection was performed as described previously [32,33]. Briefly, cryopreserved CB $CD34^+$ cells were thawed and prestimulated by incubation in StemPro-34 medium (Invitrogen, Carlsbad, CA, USA) containing cytokines at 37°C in 5% CO_2 for 24 h. Recombinant human thrombopoietin (50 ng/ml; kindly donated by Kirin Brewery, Tokyo, Japan), stem cell factor (50 ng/ml; donated by Kirin Brewery), and Flk-2/Flt-3 ligand (50 ng/ml; R&D Systems, Minneapolis, MN, USA) were used. Prestimulated $CD34^+$ cells were cultured for 12 h under the same conditions in the presence of highly concentrated lentivirus supernatant at an m.o.i. of 50. Lentivirus-infected $CD34^+$ cells were transplanted into irradiated NOG mice. The efficiency of infection was determined by FACS analysis on the day of transplantation.

Mice. NOG mice were obtained from the Central Institute for Experimental Animals (Kawasaki, Japan) and were maintained in the animal facility of the Tokai University School of Medicine in microisolator cages with autoclaved food and water. Seven- to nine-week-old NOG mice were irradiated with 250 cGy of X-rays and thereafter received acidified water containing 1.1 g/L neomycin sulfate and 131 mg/L polymyxin B sulfate (Sigma). The following day, two units of CB $CD34^+CD3^-$ cells were simultaneously injected intravenously into NOG mice. In some experiments, $CD34^-$ MNCs were cotransplanted with $CD34^+$ cells. All experiments were approved by the animal care committee of Tokai University.

Flow cytometric analysis. For kinetic analysis, mice were anesthetized with ethyl ether and PB samples were aspirated from the retro-orbital sinus. Samples were prepared as single-cell suspensions in PBS containing 0.1% human serum globulin and heparin. Human hematopoietic cells were distinguished from mouse cells by expression of human CD45. At the time of sacrifice, BM, spleen, and PB were collected for analysis of the presence of human cells by flow cytometry. BM cells were suspended in PBS using a 27-gauge needle. Spleen was teased apart, and PB was aspirated from the retro-orbital sinus. Samples were prepared as single-cell suspensions in PBS containing 0.1% human serum globulin and passed through a nylon filter to remove debris. Cells were stained with mAbs to human leukocyte differentiation antigens. APC-conjugated anti-human CD3, CD4, CD14, CD19, CD33, CD34, and CD56 mAbs (all Coulter/Immunotech) and ECD-conjugated anti-human CD8 and CD45 mAbs (all Coulter/Immunotech) were used. Four-color flow cytometric analysis was conducted using FACSVantage (BD Biosciences). Quadrants were set to include at least 97% of the isotype-negative cells. The proportion of each lineage was calculated from 20,000 events acquired using CELLQuest or FACSDiva software (BD Biosciences).

Statistical analysis. Results are expressed as individual data. Input (transplanted EGFP/EYFP ratio) and output (engrafted EGFP/EYFP ratio) were calculated by the following calculation: input (EGFP/EYFP ratio) = (EGFP transplanted cell number × infection efficiency)/(EYFP transplanted cell number × infection efficiency). Output (EGFP/EYFP ratio) = (percentage of $CD45^+EGFP^+$ cells in the recipient)/(percentage of $CD45^+EYFP^+$ cells in the recipient). The correlation of input values and output values was analyzed using StatView-J4.02 software (Abacus Concepts, Berkeley, CA, USA). P values <0.05 were considered to be significant.

Acknowledgments

We thank Hiroyuki Miyoshi, BioResource Center, RIKEN Tsukuba Institute, for the gift of lentivirus vectors; Tatsuya Sugimoto, Center for Cell Transplantation and Regenerative Medicine of Tokai University School of Medicine, for HLA typing; and members of the animal facility of Tokai University, especially Mayumi Nakagawa and Shinya Fujikawa for their meticulous care of experimental animals; and members of the Tokai Cord Blood Bank for their assistance. We also thank members of the Research Center for Regenerative Medicine of Tokai University School of Medicine for their useful discussions and assistance. This work was supported by a Research Grant-in-Aid from the Science Frontier Program from the Ministry of Education, Science, Sports, and Culture of Japan and a Sciences Research Grant from the Ministry of Health and Labor of Japan.

RECEIVED FOR PUBLICATION MARCH 26, 2004; ACCEPTED JULY 22, 2004.

References

1. Broxmeyer, H. E., *et al.* (1992). Growth characteristics and expansion of human umbilical cord blood and estimation of its potential for transplantation in adults. *Proc. Natl. Acad. Sci. USA* **89:** 4109–4113.
2. Gluckman, E., *et al.* (1989). Hematopoietic reconstitution in a patient with Fanconi's anemia by means of umbilical-cord blood from an HLA-identical sibling. *N. Engl. J. Med.* **321:** 1174–1178.
3. Gluckman, E., *et al.* (1997). Outcome of cord-blood transplantation from related and unrelated donors. *N. Engl. J. Med.* **337:** 373–381.

4. Rubinstein, P., *et al.* (1998). Outcomes among 562 recipients of placental-blood transplants from unrelated donors. *N. Engl. J. Med.* **339:** 1565–1577.
5. Gluckman, E. (2001). Hematopoietic stem-cell transplants using umbilical-cord blood. *N. Engl. J. Med.* **344:** 1860–1861.
6. Grewal, S. S., Barker, J. N., Davies, S. M., and Wagner, J. E. (2003). Unrelated donor hematopoietic cell transplantation: marrow or umbilical cord blood? *Blood* **101:** 4233–4244.
7. Weinreb, S., *et al.* (1998). Transplantation of unrelated cord blood cells. *Bone Marrow Transplant* **22:** 193–196.
8. Barker, J. N., Weisdorf, D. J., and Wagner, J. E. (2001). Creation of a double chimera after the transplantation of umbilical-cord blood from two partially matched unrelated donors. *N. Engl. J. Med.* **344:** 1870–1871.
9. Barker, J. N., Weisdorf, D. J., DeFor, T. E., Blazar, B. R., Miller, J. S., and Wagner, J. E. (2003). Rapid and complete donor chimerism in adult recipients of unrelated donor umbilical cord blood transplantation after reduced intensity conditioning. *Blood* **102:** 1915–1919.
10. Szilvassy, S. J., Humphries, R. K., Lansdorp, P. M., Eaves, A. C., and Eaves, C. J. (1990). Quantitative assay for totipotent reconstituting hematopoietic stem cells by a competitive repopulation strategy. *Proc. Natl. Acad. Sci. USA* **87:** 8736–8740.
11. Rebel, V. I., Miller, C. L., Eaves, C. J., and Lansdorp, P. M. (1996). The repopulation potential of fetal liver hematopoietic stem cells in mice exceeds that of their liver adult bone marrow counterparts. *Blood* **87:** 3500–3507.
12. Szilvassy, S. J., Weller, K. P., Chen, B., Juttner, C. A., Tsukamoto, A., and Hoffman, R. (1996). Partially differentiated ex vivo expanded cells accelerate hematologic recovery in myeloablated mice transplanted with highly enriched long-term repopulating stem cells. *Blood* **88:** 3642–3653.
13. Goerner, M., Bruno, B., McSweeney, P. A., Buron, G., Storb, R., and Kiem, H. P. (1999). The use of granulocyte colony-stimulating factor during retroviral transduction on fibronectin fragment CH-296 enhances gene transfer into hematopoietic repopulating cells in dogs. *Blood* **94:** 2287–2292.
14. Kiem, H. P., *et al.* (1997). Gene transfer into marrow repopulating cells: comparison between amphotropic and gibbon ape leukemia virus pseudotyped retroviral vectors in a competitive repopulation assay in baboons. *Blood* **90:** 4638–4645.
15. Hematti, P., Sellers, S. E., Agricola, B. A., Metzger, M. E., Donahue, R. E., and Dunbar, C. E. (2003). Retroviral transduction efficiency of G-CSF+SCF-mobilized peripheral blood CD34$^+$ cells is superior to G-CSF or G-CSF+Flt3-L-mobilized cells in nonhuman primates. *Blood* **101:** 2199–2205.
16. McCune, J. M., Namikawa, R., Kaneshima, H., Shultz, L. D., Lieberman, M., and Weissman, I. L. (1988). The SCID-hu mouse: murine model for the analysis of human hematolymphoid differentiation and function. *Science* **241:** 1632–1639.
17. Larochelle, A., *et al.* (1996). Identification of primitive human hematopoietic cells capable of repopulating NOD/SCID mouse bone marrow: implications for gene therapy. *Nat. Med.* **2:** 1329–1337.
18. Bhatia, M., Wang, J., Kapp, U., Bonnet, D., and Dick, J. E. (1997). Purification of primitive human hematopoietic cells capable of repopulating immune-deficient mice. *Proc. Natl. Acad. Sci. USA* **94:** 5320–5325.
19. Guenechea, G., Gan, O. I., Dorrell, C., and Dick, J. E. (2001). Distinct classes of human stem cells that differ in proliferative and self-renewal potential. *Nat. Immunol.* **2:** 75–82.
20. Shultz, L. D., *et al.* (1995). Multiple defects in innate and adaptive immunologic function in NOD/LtSz-scid mice. *J. Immunol.* **154:** 180–191.
21. Greiner, D. L., Hesselton, R. A., and Shultz, L. D. (1998). SCID mouse models of human stem cell engraftment. *Stem Cells* **16:** 166–177.
22. Kollet, O., *et al.* (2000). Beta2 microglobulin-deficient (B2m(null)) NOD/SCID mice are excellent recipients for studying human stem cell function. *Blood* **95:** 3102–3105.
23. Yahata, T., *et al.* (2002). Functional human T lymphocyte development from cord blood CD34$^+$ cells in nonobese diabetic/Shi-scid, IL-2 receptor gamma null mice. *J. Immunol.* **169:** 204–209.
24. Ito, M., *et al.* (2002). NOD/SCID/gamma(c) (null) mouse: an excellent recipient mouse model for engraftment of human cells. *Blood* **100:** 3175–3182.
25. Hiramatsu, H., *et al.* (2003). Complete reconstitution of human lymphocytes from cord blood CD34$^+$ cells using the NOD/SCID/gamma c null mice model. *Blood* **102:** 873–880.
26. Kim, D. W., Chung, Y. J., Kim, T. G., Kim, Y. L., and Oh, I. H. (2004). Cotransplantation of third-party mesenchymal stromal cells can alleviate single-donor predominance and increase engraftment from double cord transplantation. *Blood* **103:** 1941–1948.
27. Barker, J. N., Weisdorf, D. J., DeFor, T. E., McGlave, P. B., and Wagner, J. E. (2002). Multiple unit unrelated donor umbilical cord blood transplantation in high risk adults with hematologic malignancies: impact on engraftment and chimerism. *Blood* **100:** 41a.
28. Ormo, M., Cubitt, A. B., Kallio, K., Gross, L. A., Tsien, R. Y., and Remington, S. J. (1996). Crystal structure of the Aequorea victoria green fluorescent protein. *Science* **273:** 1392–1395.
29. Gill, R. G. (1993). T-cell–T-cell collaboration in allograft responses. *Curr. Opin. Immunol.* **5:** 782–787.
30. Hernandez-Fuentes, M. P., Baker, R. J., and Lechler, R. I. (1999). The alloresponse. *Rev. Immunogenet.* **1:** 282–296.
31. Csencsits, K. L., and Bishop, D. K. (2003). Contrasting alloreactive CD4$^+$ and CD8$^+$ T cells: there's more to it than MHC restriction. *Am. J. Transplant* **3:** 107–115.
32. Miyoshi, H., Smith, K. A., Mosier, D. E., Verma, I. M., and Torbett, B. E. (1999). Transduction of human CD34$^+$ cells that mediate long-term engraftment of NOD/SCID mice by HIV vectors. *Science* **283:** 682–686.
33. Yahata, T., *et al.* (2003). A highly sensitive strategy for SCID-repopulating cell assay by direct injection of primitive human hematopoietic cells into NOD/SCID mice bone marrow. *Blood* **101:** 2905–2913.

Available online at www.sciencedirect.com
SCIENCE DIRECT
Leukemia Research 29 (2005) 317–324
Leukemia Research
www.elsevier.com/locate/leukres

Potential and origin of the hematopoietic population in human skeletal muscle

Kosuke Tsuboi[a,b], Hiroshi Kawada[a,b,*], Eiren Toh[c], Yoon Hwan Lee[c], Mitsuyo Tsuma[b], Yoshihiko Nakamura[b], Tadayuki Sato[b], Kiyoshi Ando[a,b], Joji Mochida[c], Shunichi Kato[d], Tomomitsu Hotta[a,b]

[a] *Division of Hematology/Oncology, Department of Medicine, Tokai University School of Medicine, Bohseidai, Isehara, Kanagawa 259-1193, Japan*
[b] *Research Center for Regenerative Medicine, Tokai University School of Medicine, Kanagawa 259-1193, Japan*
[c] *Department of Orthopedic Surgery, Tokai University School of Medicine, Kanagawa 259-1193, Japan*
[d] *Department of Cell Transplantation and Regenerative Medicine, Tokai University School of Medicine, Kanagawa 259-1193, Japan*

Received 7 May 2004; accepted 13 August 2004

Abstract

While mononuclear cells isolated from murine skeletal muscle were shown to be capable of hematopoietic activity, similar hematopoietic cells (HC) recently were reported to exist in primate muscle. We investigated muscle-derived HC from young and adult human subjects. Although hematopoietic stem cells were rare in muscle, their frequency nonetheless was approximately four times greater than in peripheral blood. These cells in muscle appeared to originate from $CD45^+$ bone marrow cells. Our results suggested an additional function of human skeletal muscle as a reservoir of HC.

Keywords: Human skeletal muscle; Hematopoietic progenitors; Hematopoietic stem cells

1. Introduction

A variety of tissue-specific stem cells, including those in hematopoietic, nervous, and muscular systems, recently have been reported to have potential to differentiate into cells other than those specific to their origin. For example, hematopoietic stem cells were found capable of regenerating hepatocytes [1]; while neuronal stem cells reportedly can differentiate into hematopoietic cells [2].

Previously, investigators in several laboratories observed that cells isolated from murine skeletal muscle could carry out hematopoietic reconstitution in lethally irradiated mice [3–6]. Accordingly, we assessed the nature and origin of hematopoietic progenitors and stem cells in murine muscles using clonal cell culture and transplantation techniques [7,8]. The frequency of hematopoietic progenitors among mononuclear cells (MNC) derived from murine muscle proved 10 times greater than among MNC derived from peripheral blood (PB) [7]. Furthermore, we demonstrated that 10^5 MNC derived from murine muscle could accomplish hematopoietic engraftment in lethally irradiated recipient mice [8].

Recently a hematopoietic population also was demonstrated in primate skeletal muscle [9,10]; Mahmud et al. [9] and Jay et al. [10] reported that muscle cells isolated from human fetuses contained detectable numbers of hematopoietic progenitors. Human skeletal muscle therefore was suspected to be third source of HC in adults, in addition to BM and PB. In this study, we evaluated the nature and potential of

* Corresponding author. Tel.: +81 463 93 1121x2230; fax: +81 463 92 4511.
E-mail address: hkawada@is.icc.u-tokai.ac.jp (H. Kawada).

0145-2126/$ – see front matter © 2004 Elsevier Ltd. All rights reserved.
doi:10.1016/j.leukres.2004.08.005

hematopoietic populations derived from muscles from young and adult human subjects.

2. Materials and methods

2.1. Cell preparation

After the patients had given informed consent, skeletal muscle tissues were obtained under general anesthesia at the time of surgery to correct musculoskeletal defects (Table 1). The study protocol had been approved by the Human Research Committee of Tokai University School of Medicine. After removal of fat, epimysium, tendons, and internal connective tissue, the muscle samples were minced with scissors and incubated at 37 °C in 0.1% trypsin under constant agitation for 45 min. Cells were released from the tissue fragments by vigorous trituration. Pooled cells were filtered through a 40 μm nylon mesh, washed, and resuspended in α-modification of Eagle's medium (α-MEM; Life Technologies, Grand Island, NY). Samples were purified further by discontinuous Percoll density-gradient centrifugation (Amersham Pharmacia Biotech, Piscataway, NJ). Here, the samples were centrifuged at 15 000 g for 5 min at 8 °C in a fixed-angle rotor, and MNC were collected from the 20–60% interface. PB and BM cells also were collected from the patients during the operation. MNC were prepared from PB and BM cells by Percoll density-gradient centrifugation, as described above. In some experiments, we separated the muscle MNC into $CD45^+$ and $CD45^-$ cells using a FACS Vantage fluorescence-activated cell sorter (FACS; Becton Dickinson, San Jose, CA). For transplantation experiments, to avoid graft-versus-host disease, $CD3^+$ T-lymphocytes were depleted from the samples before transplantation using a MACS immunomagnetic separation system (Miltenyi Biotec, Glodbach, Germany).

2.2. Clonal cell culture

Methylcellulose culture was performed in 35 mm Petri dishes (Iwaki Glass, Chiba, Japan), as described previously [11]. One milliliter of culture mixture contained designated numbers of MNC, α-MEM, 1.2% 1500 cP methylcellulose (Shin-etsu Chemical, Tokyo, Japan), 1% deionized fraction V bovine serum albumin (Sigma–Aldrich, St. Louis, MO), 0.1 mM 2-mercaptoethanol (Sigma–Aldrich), 30% fetal calf serum (StemCell Technologies, Vancouver, Canada), 100 ng/mL recombinant human thrombopoietin, 100 ng/ml recombinant human stem cell factor, 3 U/mL recombinant human erythropoietin, 10 ng/mL recombinant human granulocyte-colony stimulating factor, 10 ng/mL recombinant human granulocyte/macrophage-colony stimulating factor, and 20 ng/mL recombinant human interleukin-3. All cytokines were provided by the Kirin Brewery (Tokyo, Japan). Dishes were incubated at 37 °C in a humidified atmosphere consisting of 5% CO_2 in air. Hematopoietic colonies consisting of 50 or more cells were scored using an inverted microscope after 14 days of culture. Abbreviations of colony types used here are as follows: colony-forming units in culture (CFU-C), erythroid burst-forming units (BFU-E); granulocyte and/or macrophage colonies (CFU-GM); and mixed colonies containing erythroid and myeloid cells (CFU-Mix).

2.3. Immunofluorescence photography

Cryostat sections of fresh frozen samples were fixed for 10 min at room temperature with 4% paraformaldehyde, washed in phosphate buffered saline solution (PBS), and incubated for 45 min with anti-laminin (Sigma–Aldrich). After washing in PBS sections, then were exposed for 45 min to secondary antibodies conjugated with tetramethylrhodamine isothiocyanate isomer R (Dako, Kyoto, Japan). Sections next were incubated overnight at 4 °C with biotin conjugated anti-human CD45 (BD Pharmingen, San Diego, CA), washed, and allowed to react for 4 h at 4 °C with streptavidin Alexa 488 (Molecular Probes, Eugene, OR). Then the sections were incubated for 1 h with anti-CD31 (TECHNE Corporation, Minneapolis, MN), washed, and exposed for 45 min to secondary antibodies conjugated with Alexa 594 (Molecular Probes). Nuclei were stained with TOTO-3 (Molecular Probes). Slides were examined under a confocal laser scanning microscope (LSM 510 META; Carl Zeiss, Jena, Germany).

2.4. Immunophenotyping by flow cytometry

MNC isolated from human muscle tissues were stained with FITC- or PE-conjugated monoclonal antibodies, as described previously [11]. Samples were analyzed using a FACSCalibur instrument (Becton Dickinson).

2.5. Transplantation

NOD/SCID/$\gamma c^{-/-}$ (NOG) mice 7–9 weeks old were obtained from the Central Institute for Experimental Animals (Kawasaki, Japan). All animals were handled under sterile conditions and maintained under isolation at the animal facility of Tokai University School of Medicine. Mice were sublethally X-irradiated with 250 cGy, after which they received acidified water containing 1.1 g/L neomycin sulfate and 131 mg/L polymyxin B sulfate (Sigma–Aldrich). Two hours after irradiation, the mice were transplanted with human muscle-derived cells, BM cells, or PB cells by intra-BM injection (IBM). IBM was carried out as described previously [12]. In brief, a 29-gauge needle was inserted into the joint surface of the right tibia of anesthetized mice, and human cells suspended in 30 μL of PBS were injected into the BM cavity. Mice were killed 8 weeks after transplantation, and BM cells were harvested from the femora and tibiae. The population of human hematopoietic cells was determined by detecting cells stained by FITC-conjugated anti-human CD45, using flow cytometry.

Table 1
Patients from whom samples of muscle were obtained

Patient no.	Age (years)	Gender	Underlying disease	Muscle separated (g)	MNC collected ($\times 10^5$)	Experiment
1	14	Female	Idiopathic scoliosis	Iliopsoas (5.2)	0.73	Clonal cell culture
2	55	Female	Lumbar spinal canal stenosis	Iliopsoas (2.5)	0.75	Clonal cell culture
3	34	Male	Lumbar disk herniation	Iliopsoas (5.4)	0.64	Clonal cell culture
4	65	Male	Lumbar spinal canal stenosis	Iliopsoas (4.6)	25.8	Clonal cell culture transplantation
5	7	Female	Cartilage-hair hypoplasia	External abdominal oblique (not weighed)	1.0	STR analysis
6	49	Male	Right lower leg necrosis due to diabetes mellitus	Gastrocnemius (33.0)	25.4	Clonal cell culture transplantation
7	65	Female	Chondrosarcoma at right first rib	Pectoralis major (not weighed)	Not isolated	Immunohistochemistry
8	57	Male	Leiomyosarcoma at right lower leg	Quadriceps (4.9)	1.9	FCM
9	69	Male	Lumbar spinal canal stenosis	Iliopsoas (2.4)	0.54	FCM
10	59	Female	Degenerative scoliosis	Iliopsoas (6.0)	7.77	FCM
11	32	Male	Lumbar burst fracture	Iliopsoas (7.0)	21.7	Clonal cell culture transplantation

Human muscle samples were obtained from patients after they gave their informed consent. MNC, mononuclear cells; STR, short tandem repeat; FCM, immunophenotyping by flow cytometry.

2.6. Detection of human cell engraftment in mice and donor cells in the recipient by polymerase chain reaction (PCR)

Engraftment of human cells in the BM of recipient mice also was assessed by PCR. Genomic DNA was isolated from the BM cells using standard extraction protocols. DNA (100 ng) was subjected to PCR to detect a 1171-base pair (bp) fragment of human chromosome 17-specific α-satellite using specific primers previously reported [12]. PCR was performed using an RNA PCR kit (Takara Shuzo, Tokyo, Japan). PCR products were separated on 1.0% agarose gels and visualized by ethidium bromide staining. To determine the origin of $CD45^+$ and $CD45^-$ cells in the muscle of the BM transplantation recipient, a short tandem repeat (STR) locus (ACTBP2) was amplified by PCR using specific primers previously reported [13]. PCR products were separated using the 310 Genetic Analyzer (Applied Biosystems, Foster City, CA, USA).

2.7. Statistical analysis

Student's *t*-test was used to determine the statistical significance of differences.

3. Results

3.1. Hematopoietic populations in human muscle

We first assessed the nature of hematopoietic populations in human muscle tissue. We cultured MNC isolated from muscle in methylcellulose, and compared these cells with MNC isolated from PB. The frequency of CFU-C in muscle-derived MNC was approximately four times greater than in PB-derived MNC ($P < 0.05$, Fig. 1A). The majority of colonies grown from the muscles were CFU-GM or BFU-E. However, CFU-Mix also were observed (Fig. 1A and B). The number of CFU-GM in muscle was significantly higher than in PB ($P < 0.05$). These results indicated that a distinct hematopoietic population indeed exists in human muscle.

We further separated muscle-derived MNC into $CD45^+$ cells and $CD45^-$ cells by FACS, and aliquots were cultured separately in methylcellulose, since $CD45^-$ muscle cells isolated from human fetuses were reported to contain assayable hematopoietic progenitors [9,10]. Fourteen days later, hematopoietic colonies were detected in dishes in which $CD45^+$ cells were cultured (Table 2). On the other hand, the $CD45^-$ fraction contained no cells capable of forming hematopoietic activity in vitro.

We then set out to localize the hematopoietic population in the muscle tissue. Although some $CD45^+$ cells were found in vessels, the majority of $CD45^+$ cells were located outside of vessels (Fig. 2a). Extravascular $CD45^+$ cells were 24 times as numerous as $CD45^+$ cells in the vessels. Most $CD45^+$ cells, including $CD45^+CD34^+$ cells, were observed in the interstitial space between muscle fibers in the skeletal muscle specimens (Fig. 2a and b).

The phenotype of muscle MNC also was analyzed by flow cytometry. Approximately half of the cells were positive for CD45, and most $CD45^+$ cells expressed lineage-specific markers (Table 3). However, $CD45^+CD34^+$ cells were also found in muscle, and approximately half of these lacked lineage-specific markers (data not shown).

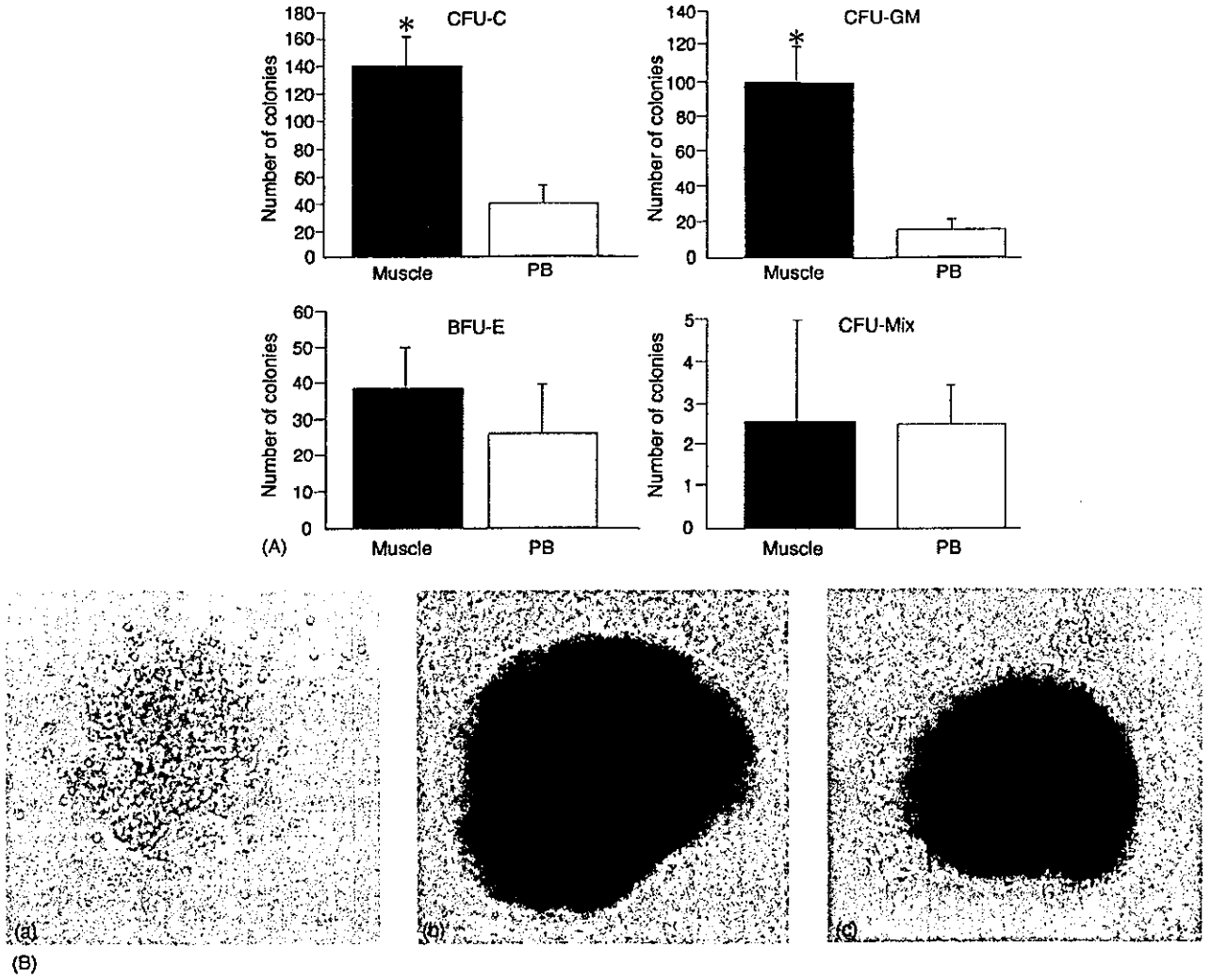

Fig. 1. Formation of hematopoietic colonies by mononuclear cells (MNC) derived from human muscles and peripheral blood (PB). (A) Comparison of colony formation by MNC derived from muscles and PB. From six patients (patients 1–4, 6, and 11 in Table 1), MNC were isolated from muscle and PB, and 2×10^5 muscle MNC and 8×10^5 PB MNC were plated in quadruplicate in the presence of hematopoietic cytokines. On day 14 of culture, colonies were counted. Bars represent the mean and standard deviation for the results obtained from 8×10^5 MNC in the six samples. $^*P < 0.05$ compared with PB. No significant differences were evident in BFU-E or CFU-Mix between muscle and PB. (B) Representative hematopoietic colonies from human muscle. (a) CFU-GM, (b) BFU-E, (c) CFU-Mix.

Table 2
Comparison of colony formation between $CD45^+$ cells and $CD45^-$ cells separated from muscle mononuclear cells (MNC)

Patient no.	Cells	Hematopoietic colony			
		GM	BFU-E	GEMM	Total[a]
4	$CD45^+$ (4×10^4/dish)	5 ± 1	2 ± 1	0	7 ± 1
	$CD45^-$ (6×10^4/dish)	0	0	0	0
6	$CD45^+$ (5×10^4/dish)	5 ± 2	2 ± 1	1 ± 1	8 ± 2
	$CD45^-$ (5×10^4/dish)	0	0	0	0
11	$CD45^+$ (2×10^4/dish)	2 ± 1	1 ± 1	0	3 ± 1
	$CD45^-$ (2×10^4/dish)	0	0	0	0

$CD45^+$ cells and $CD45^-$ cells were separated by FACS sorting from muscle MNC of the patients (numbers 4, 6, and 11 in Table 1). Fractionated cells were plated in quadruplicate in the presence of hematopoietic cytokines. The number of cells plated per dish was proportional to the number of $CD45^+$ and $CD45^-$ cells among the MNC. On day 14 of culture, colonies were assessed by observation under an inverted microscope. Data represent the mean and standard deviation of values obtained from four dishes.

[a] Total number of colonies.

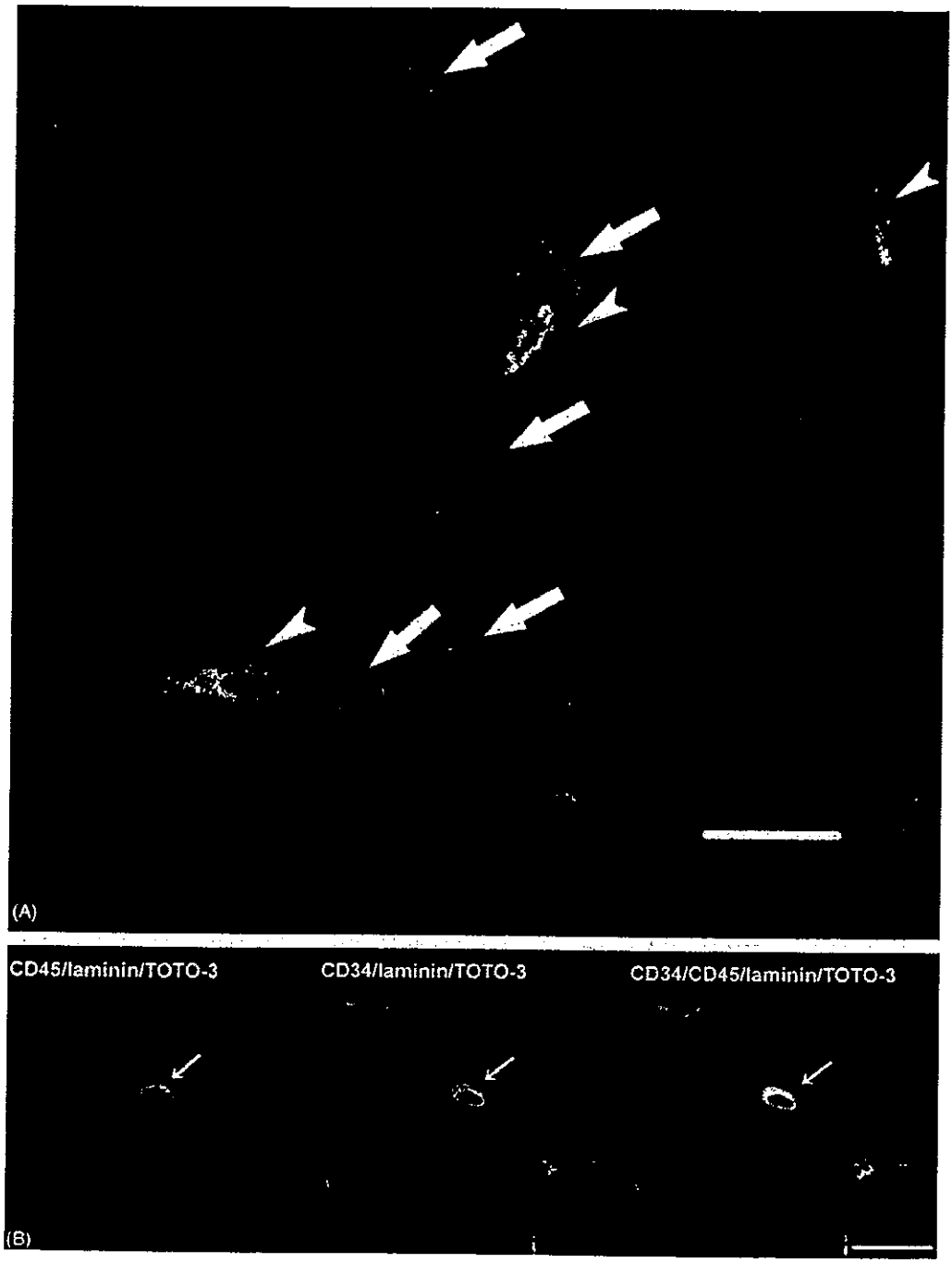

Fig. 2. Localization of hematopoietic cells in human muscle. (a) In muscle, $CD45^+$ cells were observed in the interstitial space between muscle fibers. Green, red, orange, and blue signals indicate CD45, laminin, CD31, and TOTO-3, respectively. Arrows indicate $CD45^+$ cells, and arrowheads indicate vessels in the interstitium of the muscle. Most $CD45^+$ cells were extravascular. Bar indicates 20 μm. (b) $CD45^+CD34^+$ cells also were observed in the interstitial space between muscle fibers. The representative result is shown. Green, orange, red, and, blue signals indicate CD45, CD34, laminin, TOTO-3, respectively. Bar indicates 20 μm.

Table 3
Phenotypes of human muscle cells

Phenotype	Positive cells (%)[a]
$CD45^+$	49 ± 11
$CD45^+CD34^+$	3 ± 2
$CD45^+CD31^+$	2 ± 1
$CD45^+CD38^+$	14 ± 7
$CD45^+CD3^+$	28 ± 16
$CD45^+CD19^+$	7 ± 3
$CD45^+CD13/14/33^+$[b]	11 ± 7
$CD45^-CD34^+$	14 ± 4
$CD45^-CD31^+$	6 ± 2
$CD45^-CD38^+$	3 ± 1
$CD45^-CD3/19/13/14/33^+$[c]	0

Phenotypes of mononuclear cells derived from human muscles were assessed by flow cytometry. Approximately, half of the muscle cells were positive for CD45.

[a] Data are the mean ± standard deviation for three different experiments.

[b] $CD45^+$ cells expressing CD13, CD14, or CD33.

[c] $CD45^-$ cells expressing CD3, CD19, CD13, CD14, or CD33.

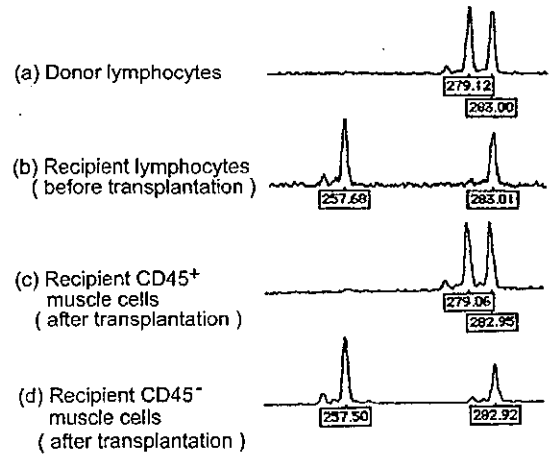

Fig. 3. Origin of the hematopoietic population in muscles from a patient treated with bone marrow (BM) transplantation. DNA collected from donor and recipient cells was amplified using the ACTBP2 locus-specific primer, and automatically analyzed by an ABI 373A sequencer using Genescan software 672, following electrophoresis on a 6% denaturing polyacrylamide gel. Numbers indicate base pairs (bp). All $CD45^+$ cells from recipient muscle showed the donor genotype, indicating BM origin.

3.2. Origin of the hematopoietic population in human muscle

Next we examined the origin of the hematopoietic population in the muscle. MNC were isolated from muscle of a patient previously diagnosed with cartilage-hair hypoplasia, a congenital malformation associated with immunodeficiency, and had undergone allogenic BM transplantation at the age of 4 years from an unrelated healthy donor selected through the Japan Marrow Donor Program, 3 years previously (patient no. 5 in Table 1). The preconditioning regimen for transplantation had been thoraco-abdominal irradiation followed by cyclophosphamide and anti-thymocyte globulin. We divided the muscle MNC into $CD45^+$ cells and $CD45^-$ cells by FACS, and subjected them to analysis of STR polymorphism. If $CD45^-$ recipient muscle cells could differentiate into hematopoietic cells, some of the $CD45^+$ cells in the muscles should show the recipient genotype. However, all $CD45^+$ cells in the muscle showed the donor genotype, while all $CD45^-$ cells showed the recipient genotype (Fig. 3b). These results indicated that the hematopoietic cells in the muscles were derived from BM, and that $CD45^-$ cells did not differentiate into hematopoietic cells in vivo.

3.3. Engrafting capabilities of MNC isolated from human muscle

We tested the hematopoietic engrafting capabilities of MNC derived from human muscle by transplantation into immunodeficient mice. In previous studies, all (5/5) congenic recipient mice transplanted with 10^5 MNC derived from murine muscles showed hematopoietic engraftment, while only one-fourth of the mice transplanted with 10^4 of the same cells showed hematopoietic engraftment [8]. Therefore, for this study, we decided to use more than 10^5 human MNC for transplantation experiments. Furthermore, we chose NOG mice as the recipients and used IBM injection for transplantation, because these mice were previously demonstrated to be 10 times more sensitive for SCID-repopulating cell assay than NOD/SCID mice, while IBM injection also was considered to be a strategy 15 times more sensitive for the SRC assay than intravenous injection [12,14].

MNC (5×10^5 cells) derived from muscle, BM, or PB were transplanted separately into irradiated NOG mice by IBM injection. Additionally, we separated 5×10^5 muscle-derived MNC into $CD45^+$ cells and $CD45^-$ cells by FACS; and these cells also were transplanted into recipient mice. Eight weeks later, BM cells were collected from the recipient mice, and levels of engraftment were analyzed by flow cytometry. As expected, human $CD45^+$ cells were detected in mice transplanted with BM-derived MNC. However, we did not detect human $CD45^+$ cells in mice transplanted with muscle-derived MNC, $CD45^+$ cells, or $CD45^-$ cells, or PB-derived MNC (data not shown).

We also examined BM samples collected from recipient mice by PCR. Here again, engraftment of human cells was recognized in mice transplanted with PB-derived MNC (Fig. 4), but not in mice transplanted with muscle-derived MNC or $CD45^+$ cells. Interestingly, engraftment was detected at a very low percentage in one mouse transplanted with muscle-derived $CD45^-$ cells. Since no human $CD45^+$ cells were detected in the BM of recipient mice by flow cytometry (data not shown), human $CD45^-$ cells were considered to have engrafted in this mouse as a non-hematopoietic population, although we could not determine the phenotype of the engrafted cells.

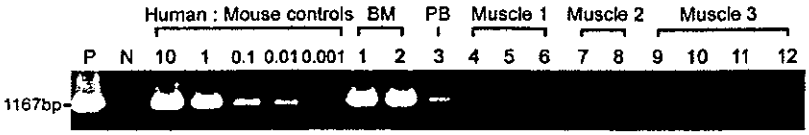

Fig. 4. Polymerase chain reaction (PCR) analysis of bone marrow (BM) samples from individual NOD/SCID/$\gamma c^{-/-}$ (NOG) mice transplanted with human muscle-, peripheral blood (PB)-, or BM-derived mononuclear cells (MNC). Five hundred thousand MNC derived from human muscle, PB, or BM were transplanted separately into irradiated NOG mice by intra-BM injection. PB, BM, and Muscle 1-derived cells were isolated from patient 4 in Table 1. Muscle 2- and Muscle 3-derived cells were from patients 6 and no. 11, respectively. Lanes 1–12 represent results obtained from individual recipient mice. Muscle 3-derived cells (5×10^5 MNC) were separated further into $CD45^+$ (lanes 9 and 10) and $CD45^-$ cells (lanes 11 and 12), and these cell fractions then were transplanted separately into mice. Eight weeks after transplantation, DNA was extracted from recipients BM cells, and engraftment was assessed by PCR. Human: mouse DNA controls are designated by the percentage of human DNA. P, positive control; N, negative control.

4. Discussion

In this study, we sought to characterize the hematopoietic population in muscle of young and adult human subjects. We first demonstrated that the frequency of hematopoietic progenitors in muscle tissue differed from that in PB. We clarified that these hematopoietic cells were derived from $CD45^+$ cells. The presence of enriched numbers of hematopoietic progenitors in the muscle cannot be explained as contamination by blood cells. In fact, most hematopoietic cells had an extravascular location in the muscle. However, they appeared to have originally arisen from BM. These results are essentially compatible with those of previous studies in mice [7,8,15,16], but HSC activity was not detected in adult human muscle by IBM injection of 5×10^5 MNC into NOG mice. Taking the present results together with those of clonal cell culture, we considered most of the hematopoietic population in the muscle to be at the progenitor level and that HSC, if present at all, were much rarer in human than mouse muscle [8]. Dose escalation studies or further enrichment of HSC might provide further information regarding HSC activity in human muscle, although obtaining sufficiently large samples would be difficult.

Although little is known about differentiation potential in human stem cells, several reports demonstrated that plasticity phenomena also could be recognized in human adults [17,18]. Clinical applications of stem cell plasticity therefore have been expected in the field of regenerative medicine. However, in this study, we demonstrated that muscle-derived $CD45^-$ cells from young or adult human subjects were not capable of differentiating into hematopoietic cells in vitro and in vivo, in contrast to the reported result that $CD45^-$ cells from fetal human muscle could differentiate into hematopoietic cells [10]. These findings were compatible with the results of Mahmud et al. [9], who showed that $CD45^-$ cells isolated from the muscles of adult baboons did not show hematopoietic activity; the same result also was obtained in mice [8]. The hematopoietic potential of muscle-derived $CD45^-$ cells might be limited to the fetal and neonatal periods [9,10,19]. However, Howell et al. [19] reported that hematopoietic colony-forming activity and engraftment potential of muscle-derived $CD45^-$ cells from neonatal mice were induced or increased by cell culture. Furthermore, Dell'Agnola et al. [20] recently reported that cultured human stem cells residing in adult muscle showed hematopoietic engraftment in immunodeficient mice, while noncultured human stem cells did not. Since ex vivo expansion of human BM-derived HSC has been difficult to attain so far, in vitro culture might recruit extra-functions of cells residing in adult muscular tissues.

In conclusion, we demonstrated a unique hematopoietic population in human skeletal muscle. Our results indicated that while human muscle is not expected to be an HSC source in the clinical settings, skeletal muscles collectively constitute the largest organ in the human body and contain hematopoietic progenitors at higher frequency than peripheral blood. Therefore, human skeletal muscle, an organ specializing in movement, also could function as a reservoir of hematopoietic cells in addition to BM and spleen.

Acknowledgements

The authors thank Drs. Yukiharu Yasuda and Takashi Shimizu, and the staff members of the Department of Orthopedic Surgery, Tokai University School of Medicine for collecting the tissue samples, Fumiko Tsuchida for STR analysis, and Drs. Takashi Yahata and Yukari Muguruma for useful advice and discussion. This work was supported by the Sagawa Foundation for Promotion of Cancer Research, 2002 Tokai University School of Medicine Research Aid, and a Research Grant from the Science Frontier Program from the Ministry of Education, Science, Sports, and Culture of Japan.*Contributions*. Kosuke Tsuboi contributed to the concept and design, and collected and assembled the data. Hiroshi Kawada contributed to the concept and design, and analyzed and interpreted the data. Eiren Toh, Yoon Hwan Lee, and Shunichi Kato, analyzed and interpreted the data, and also provided study materials or access to patients. Mitsuyo Tsuma, Yoshihiko Nakamura, and Tadayuki Sato analyzed and interpreted the data. Kiyoshi Ando, Joji Mochida, and Tomomitsu Hotta analyzed and interpreted the data, and provided administrative support.

References

[1] Lagasse E, Connors H, Al-Dhalimy M, Reitsma M, Dohse M, Osborne L, et al. Purified hematopoietic stem cells can differentiate into hepatocytes in vivo. Nat Med 2000;6:1229–34.